Acta Astronautica 200 (2022) 462–477

Contents lists available at ScienceDirect

Acta Astronautica

journal homepage: www.elsevier.com/locate/actaastro

Research Paper

All-At-Once formulation integrating pseudo-spectral optimal control for launch vehicle design and uncertainty quantification

Mathieu Balesdent [a,*], Loïc Brevault [a], Jorge-Luis Valderrama-Zapata [a,b], Annafederica Urbano [b]

[a] ONERA/DTIS, Université de Paris-Saclay, Palaiseau, France
[b] ISAE-Supaero, Université de Toulouse, Toulouse, France

ARTICLE INFO

Keywords:
Multidisciplinary design and optimization
Uncertainty quantification
Optimal control
Pseudo-spectral approaches
Launch vehicle design

ABSTRACT

Launch vehicle design is a multidisciplinary process involving different disciplines such as aerodynamics, structure, propulsion and trajectory. This latter is a key discipline in the design process as it is used to assess the overall performance of the vehicle by solving of an optimal control problem involving a system of nonlinear ordinary differential equations. Usual Multidisciplinary Design Optimization methods for launch vehicle design consider the trajectory design discipline as an auxiliary embedded optimization problem to find the optimal trajectory control. In this paper, a multidisciplinary approach is proposed relying on an All-At-Once formulation by using Gauss–Lobatto collocation technique to solve the optimal control problem. The problem is solved using a gradient-based optimizer. Furthermore, based on this framework, an uncertainty quantification technique using post-optimality analysis is derived to perform sensitivity analysis. This allows to analyze the influence of modeling uncertainty on the optimal launch vehicle performance in the early design phases. The efficiency of the proposed approach is illustrated on the optimization and uncertainty quantification of a representative Two-Stage-To-Orbit launch vehicle design problem.

1. Introduction

Launch Vehicle Design (LVD) often consists in finding best architectures that allow to obtain the maximum performance at the lowest possible cost for injecting a given payload in a target orbit. In pursuing these aims, LVD involves multidisciplinary processes to model all the different disciplines (*e.g.*, structure, performance, aerodynamics) that are required to assess the performance and reliability of the explored configurations [1]. These disciplines of LVD are strongly linked to each other as LVD considers the launcher as a whole, and changes in one discipline can greatly influence the others. As an example, let consider two typical disciplines in LVD, like structure and trajectory. On one side, the structure discipline is in charge of computing the mass of the different systems composing the launcher considering the loads undertaken during the flight. On the other side, the trajectory discipline is in charge of computing the altitude, the attitude (*e.g.*, flight path angle, angle of attack) and the velocity profiles that the vehicle must follow to fulfill the requirements of a given mission [2]. A trajectory has a maximum dynamic pressure point that dictates the maximum aerodynamic forces experienced by the launcher. The stronger these aerodynamic loads, the stronger the launcher should be to withstand them, hence increasing its structural mass. If the initial mass of the vehicle changes, the path, and velocity profile followed will change too. As the velocity profile changes, the maximum dynamic pressure changes; thus, the structure (and therefore the mass) required for the launcher to withstand the loads will change. The resultant dependency loop between both disciplines is an example of the intricate interactions that are solved during the design process while trying to reach an optimal solution.

The trajectory assessment is one of the key disciplines in LVD. Indeed, this discipline is mainly responsible for the performance assessment (*e.g.* minimization of the total mass, maximization of the payload mass, minimization of the propellant consumption). This discipline often involves an optimal control problem that can be transcribed as an embedded optimization problem to solve (*i.e.*, given a specific LV architecture candidate, finding the optimal control law in order to optimize the launch vehicle performance). This optimal control problem requires to solve an Ordinary Differential Equations (ODE) system that can be computationally intensive. Betts introduced a compendium of methods for trajectory optimization for a defined launch vehicle architecture in Betts [3,4]. Rao did the same for optimal control in Rao [5] and defined trajectory optimization problems as a subset of optimal control where the input design parameters are static. Thus, dealing with the optimization of parametric functions whereas in the more general case Optimal Control is related to functional optimization problems (infinite

* Corresponding author.
E-mail address: mathieu.balesdent@onera.fr (M. Balesdent).

https://doi.org/10.1016/j.actaastro.2022.08.032
Received 10 May 2022; Received in revised form 21 July 2022; Accepted 17 August 2022
Available online 22 August 2022

dimension problems). Two main classifications can be done for optimal control methods: indirect methods and direct methods. The choice of the optimal control strategy has a direct impact on the performance of the multidisciplinary design process. Indeed, as described in Section 2, indirect methods are more efficient but suffer of a lack of robustness to the initialization that can be problematic when the domain of variation of the design variables is large. In this paper, the terms optimal control and trajectory optimization are used in-distinctively.

Regarding the LVD process, in a classical design approach, individual optimization of each discipline (*e.g.*, aerodynamics, structure, trajectory, propulsion) can be carried out to determine the optimal values of the design variables (*e.g.,* propellant masses, combustion chamber pressure, stage diameters). Consequently, the optimum results are transferred from one discipline to the other disciplines in an iterative process. This approach presents difficulties to consider all of the complex interactions between the different disciplines, thus yielding sub-optimal results at the system-level [1]. In the quest for designing more efficient and lower-cost launch vehicles, Multidisciplinary Design Optimization (MDO) approaches have been used to better assess the complex interactions among disciplines during the optimization process. The most common MDO approach for LVD is MultiDiscipline Feasible (MDF) [6]. In this method, the design variables for all disciplines are driven by a unique optimizer in a single level process. At each iteration of the optimizer, the consistency of the interdisciplinary coupling variables is guaranteed by solving a MultiDisciplinary Analysis (MDA) with a fixed point iteration or a Newton solver [7].

MDO formulations can be classified according to the number of optimizers required as single-level (also called monolithic [7]) or multi-level techniques (also called distributed). In this paper, a new single-level MDO approach for LVD is proposed to reduce the computational cost of traditional methods. It relies on the single-level All-At-Once (AAO) formulation [8] and involves pseudo-spectral method to perform the trajectory optimization, with analytical gradient calculation. In the proposed approach, the design variables, the interdisciplinary coupling variables, and the variables associated with the transcribed optimal control problem are driven by the same optimizer, eliminating the nested loops and reducing the number of calls to the disciplines. It allows to parallelize the discipline evaluations and to propagate derivatives in the whole design process and to use specific gradient-based optimizers to solve the global MDO problem at a reduced computational cost.

In early design phases of launch vehicles, simplified disciplinary models are often used in order to explore large design space at a controlled numerical cost [9]. These models are characterized by a reduced computational cost but with a large level of uncertainty (*e.g.*, due to numerical approximations, physical simplifications). For instance, for aerodynamics, CFD Euler simulation may be used instead of CFD RANS. For propulsion simplified thermodynamics model for the propellant combustion and the estimation of the engine specific impulse could be employed. These uncertainties have to be assessed in order to ensure that the found optimal architecture stays valid in the further design phases when the disciplinary models will be refined with higher fidelity models. For that purpose, Uncertainty Quantification (UQ) techniques can be used [10]. UQ consists of a collection of mathematical methods to model, propagate and analyze the impact of uncertainties [11]. Among all the UQ methods, the sensitivity analysis techniques allow to apportion the uncertainty observed in the system performances to the different sources of the uncertainties [12]. This enables, for instance, to identify the uncertain parameters with almost no influence and to freeze them to nominal values, thus reducing the dimensionality for UQ studies. It also allows to identify the uncertainties that have a great influence and need to be further investigated. Different sensitivity analysis techniques may be used such as Morris technique [13], Sobol' indices [14], HSIC indices [15], *etc.* For more details about sensitivity analysis, one may consult [16]. In the context of MDO process with the use of gradient-based methods, the Derivative-based Global Sensitivity Measures (DGSM) are interesting sensitivity measures [17] because they exploit the derivatives of system performances with respect to the uncertain parameters to compute global sensitivity indices. In this paper, a methodology to compute these indices is proposed by coupling the proposed AAO formulation with post-optimality analysis [18] to efficiently calculate the derivatives of the system performance with respect to uncertain parameters at the optimal values of the design variables found by the MDO gradient-based strategy. The sensitivity measures may provide a first order of magnitude of the influence of the uncertain parameters on the resulting launch vehicle performances.

The remainder of the paper is organized as follows. In Section 2, a focus is made on the formulation of the trajectory optimization problem and the different techniques that can be used for LV optimal control problems. Section 3 deals with the formulation of the launch vehicle MDO problem. In Section 4, the proposed formulation coupling AAO and pseudo spectral control for both optimization and uncertainty quantification is described. Finally, this formulation is applied on a Two-Stage-To-Orbit LV design problem in Section 5 to compare its performance with respect to a classical MDO formulation.

2. Launch vehicle trajectory optimization

Launch vehicle design defines a particular engineering design problem because the estimation of its performance (*e.g.*, mass of the payload into orbit, estimation of Gross-Lift-Off-Weight for a given payload) is often carried out by solving a trajectory optimization problem. Indeed, in the launch vehicle design process, the trajectory discipline plays a key role and often drives the design process [1]. In this section, the main methods for solving optimal control problems for a launch vehicle are introduced. Trajectory optimization problem for launch vehicle may be solved using direct or indirect methods to find the optimal control law that minimizes a performance criterion while satisfying the path constraints [3]. Typically, the trajectory of launch vehicle can be described as the evolution in time of some state variables (*e.g.*, altitude, velocity, flight path angle). It follows a system of Ordinary Differential Equations (ODEs) to be integrated which represents the equations of motion:

$$\dot{\mathbf{x}}(t) = f_{\text{ode}}(\mathbf{x}(t), \mathbf{w}(t))$$

with $\mathbf{x}$ the state vector, t the time, f_{ode} the equations of motion and $\mathbf{w}$ the control law (for example the pitch angle profile as a function of time). To define this control law, the trajectory is optimized with respect to a given criterion $J(\mathbf{x}(t), \mathbf{w}(t))$ (*e.g.*, duration of the flight, propellant consumption, mass of payload). Furthermore, different constraints $\mathbf{g}_{\text{path}}(\mathbf{x}(t), \mathbf{w}(t))$ can be considered during the flight (*e.g.*, maximal dynamic pressure, maximal aerothermal flux). Thus, the generic optimal control problem may be expressed as :

$$\begin{aligned}
\min \quad & J(\mathbf{x}(t), \mathbf{w}(t)) && \text{(1a)}\\
\text{w.r.t.} \quad & \mathbf{w}(t) && \\
\text{s.t.} \quad & \dot{\mathbf{x}}(t) = f_{\text{ode}}(\mathbf{x}(t), \mathbf{w}(t)) && \text{(1b)}\\
& \mathbf{g}_{\text{path}}(\mathbf{x}(t), \mathbf{w}(t)) \leq 0 && \text{(1c)}\\
& \mathbf{x}_{\mathbf{min}} \leq \mathbf{x}(t) \leq \mathbf{x}_{\mathbf{max}} \quad \forall t \in \mathcal{T} && \text{(1d)}\\
& \mathbf{w}_{\mathbf{min}} \leq \mathbf{w}(t) \leq \mathbf{w}_{\mathbf{max}} \quad \forall t \in \mathcal{T} && \text{(1e)}\\
& \mathbf{x}(t_0) = \mathbf{x}_0 && \text{(1f)}\\
& \mathbf{x}(t_f) = \mathbf{x}_f && \text{(1g)}
\end{aligned}$$

where $\mathcal{T}$ is the time domain, t_0 and t_f are the initial and final times of the trajectory and $\mathbf{x}(t_0) = \mathbf{x}_0$ is in general defined by the trajectory initialization. The state and control variable vectors are defined within an interval with corresponding lower and upper bounds. Two main categories of optimization techniques may be distinguished to solve such an optimization trajectory problem [3,5]. These are the indirect and the direct methods. These methods are described in the following sections.

2.1. Indirect methods

Considering the optimal control defined previously, the augmented Lagrangian of the optimization problem can be formulated as follows:

$$L(\mathbf{x}(t), \mathbf{w}(t), \boldsymbol{\mu}, \boldsymbol{\mu}_f, \lambda) = J(\mathbf{x}(t), \mathbf{w}(t)) + \boldsymbol{\mu}^T \mathbf{g}_{\text{path}}(\mathbf{x}(t), \mathbf{w}(t)) + \boldsymbol{\mu}_f [\mathbf{x}(t_f) - \mathbf{x}_f] + \int_{t_0}^{t_f} \lambda^T [\dot{\mathbf{x}}(t) - f_{\text{ode}}(\mathbf{x}(t), \mathbf{w}(t))] \mathrm{d}t \quad (2)$$

where $\boldsymbol{\mu}$, $\boldsymbol{\mu}_f$ are the Lagrange multipliers associated to the constraints, and λ the costate vector. The Hamiltonian of the problem is defined as:

$$H(\mathbf{x}(t), \mathbf{w}(t), \lambda) = \lambda^T f_{\text{ode}}(\mathbf{x}(t), \mathbf{w}(t)) \quad (3)$$

Following the Pontryagin Maximum Principle [19], indirect techniques analytically construct the necessary and sufficient conditions for optimality based on the calculus of variations and the formulation of first-order optimality conditions on the Hamiltonian for the optimization problem (forming the Hamiltonian Boundary Value Problem) [20]. These optimality conditions are written as follows (for the sake of conciseness, the optimality conditions are only mentioned for optimal control problems with no path constraints, for more details about generic inequality constraints, one can consult [21]):

$$\dot{x}(t) = \frac{\partial H(\mathbf{x}(t), \mathbf{w}(t), \lambda)}{\partial \lambda} = H_{\lambda}(\mathbf{x}(t), \mathbf{w}(t), \lambda) \quad (4a)$$

$$\dot{\lambda}(t) = \frac{\partial H(\mathbf{x}(t), \mathbf{w}(t), \lambda)}{\partial \mathbf{x}} = -H_{\mathbf{x}}(\mathbf{x}(t), \mathbf{w}(t), \lambda) \quad (4b)$$

$$\mathbf{w}(t) = \underset{\mathbf{v}}{\operatorname{argmin}} \; H(\mathbf{x}(t), \mathbf{v}, \lambda) \quad (4c)$$

$$\mathbf{x}(t_0) = \mathbf{x}_0 \quad (4d)$$

$$\mathbf{x}(t_f) = \mathbf{x}_f \quad (4e)$$

Classically, this problem involves a shooting method which consists in finding the initial values of the co-state vector, the Lagrange multipliers, and the final time t_f to satisfy the previous equations using a Newton–Raphson method for instance. These methods are called indirect as they solve the problem indirectly by converting the optimal control problem to a boundary-value problem. Indirect methods are very precise but also very sensitive to the initial guess (associated to the co-state vector) and therefore difficult to use within the context of MDO [1] as the whole launcher is modified along the optimization process by also optimizing the architectural design variables (*e.g.*, stage diameter, chamber pressure, nozzle geometry).

2.2. Direct methods

Direct methods discretize the trajectory optimization problem directly, converting it into a constrained parametric optimization problem and then it is solved using a NLP (Non Linear Programming) optimizer. These methods are often used in the MDO context as the architecture of the launcher is optimized along with its trajectory [1], as it will be described in the following sections. The transcription of a trajectory is the process by which a trajectory optimization problem is mapped into a parametric optimization problem. This is sometimes referred to as discretization. Transcription methods generally fall into two categories: direct shooting methods and collocation methods and are described in the next sections.

2.2.1. Direct single shooting technique for trajectory optimization

The direct single shooting technique [3] is one of the most used direct methods for launch vehicle trajectory optimization. The transcription of the optimal control problem into a parametric optimization problem is done by discretizing the control law in time of the launch vehicle using a finite set of parameters $\mathbf{w}_{p_i}$, $i = 1, \ldots, n$ which are controlled by the optimizer to meet the optimality conditions. Therefore, the control law $\mathbf{w}(t, \mathbf{w}_{p_i})$ is a function of time t and of the control parameters $\mathbf{w}_{p_i}$. The problem transcription leads to the solving of a two-point boundary problem by using an initial guess for the trajectory control parameters $\mathbf{w}(t, \mathbf{w}_{p_i})$. The single shooting technique uses a numerical iterative method (such as Runge–Kutta) to integrate the ordinary differential system of equations (ODE) that represents the equations of motion (EoM) (Fig. 1). The state variables at the final time are compared with the final boundary conditions and the path constraints are evaluated. The NLP optimizer uses this information to identify a new guess for the trajectory control parameters that allows to meet the optimality conditions. This optimization problem may be expressed as:

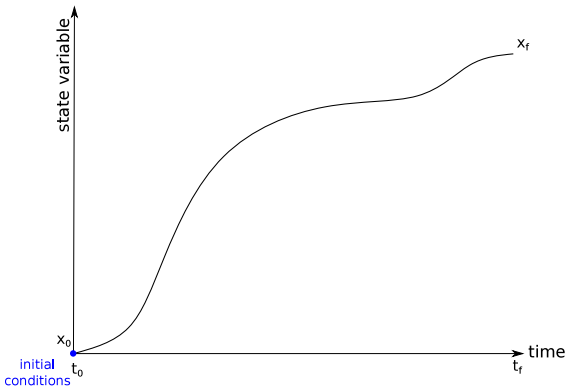

Fig. 1. Single shooting technique for launch vehicle trajectory.

$$\begin{aligned}
&\min \quad J\left(\mathbf{x}(t), \mathbf{w}\left(t, \mathbf{w}_{p_i}\right)\right) && (5a)\\
&\text{w.r.t.} \quad \mathbf{w}_{p_{i=1,\ldots,n}} && \\
&\text{s.t.} \quad \dot{\mathbf{x}}(t) = f_{\text{ode}}\left(\mathbf{x}(t), \mathbf{w}\left(t, \mathbf{w}_{p_i}\right)\right) && (5b)\\
&\qquad \mathbf{g}_{\text{path}}\left(\mathbf{x}(t), \mathbf{w}\left(t, \mathbf{w}_{p_i}\right)\right) \leq 0 && (5c)\\
&\qquad \mathbf{x}_{\mathbf{min}} \leq \mathbf{x}(t) \leq \mathbf{x}_{\mathbf{max}} \quad \forall t \in \mathcal{T} && (5d)\\
&\qquad \mathbf{w}_{\mathbf{min}} \leq \mathbf{w}_{p_i} \leq \mathbf{w}_{\mathbf{max}} \quad \forall t \in \mathcal{T} && (5e)\\
&\qquad \mathbf{x}(t_0) = \mathbf{x}_0 && (5f)\\
&\qquad \mathbf{x}(t_f) = \mathbf{x}_f && (5g)
\end{aligned}$$

This optimization problem may be solved either using gradient-based algorithms or evolutionary algorithms. It is in general a low-dimensional optimization problem (few dozen of optimization variables). As an ODE integrator (*e.g.,* Runge–Kutta integrator) is used starting form initial conditions ($\mathbf{x}(t_0) = \mathbf{x}_0$), at each iteration of the optimizer, the launcher trajectory is physically relevant as it follows the EoM. One of the difficulties with gradient-based optimizers is the need to compute the gradients, often using finite difference approximations which implies as many trajectory simulations as the number of parameters defining the control law. Moreover, the final state variables are very sensitive to small perturbations of the control law parameters due to the numerical integration process. The main difficulty is that small variations on control law parameters occurring at the beginning of the trajectory may be accentuated all along the trajectory and so may lead to harmful effects such as trajectory divergence. This phenomenon is increased by the highly non-linear nature of the dynamics function $f_{\text{ode}}(\cdot)$. Eventually, gradient-based optimizers only ensure local convergence which could lead to repeated problem solvings with different initializations (multi-start techniques) when multiple minima are present. Evolutionary algorithms allow for global convergence but in general result in a high number of trajectory simulation evaluations.

2.2.2. Pseudo-spectral technique for trajectory optimization

The collocation techniques [22] consist in discretizing the dynamics in time and replacing the dynamic equations (state and control dynamics) by piece-wise continuous polynomials in order to transcribe

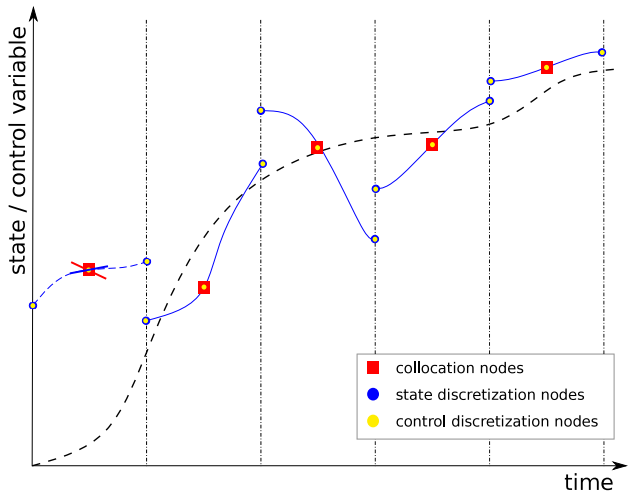

Fig. 2. Example of pseudo-spectral technique for launch vehicle trajectory, here the Legendre–Gauss–Lobatto of order 3 (on the first segment, slopes are indicated for the collocation node).

the optimal control problem into a NLP problem (Fig. 2). There exist local and global collocation techniques. Global collocation methods are also called pseudo-spectral. In local orthogonal collocation, the induced discretization error can be reduced by varying the number of discretization segments and fixing the interpolating polynomial degree, whereas the inverse approach (*i.e.*, increasing the polynomial degree and fixing the number of discretization segments)is followed for the pseudo-spectral approaches. The interest for global collocation approach is the spectral convergence (exponential rate) as a function of the number of collocation points.

In collocation methods, the coefficients of an interpolating polynomial are calculated simultaneously and are constrained to match the ODE at the collocation points when approximating the solution of the equations. Different techniques such as Gauss, Radau and Lobatto methods exist and their differences are based on the inclusion or not of endpoints on the current interval. A subset of these methods is orthogonal collocation which uses orthogonal polynomials to approximate the functions, typically Chebyshev or Legendre polynomials, but also Jacobi polynomials for a High-Order Gauss–Lobatto method. Defect constraints are added to the optimization problem in order to ensure the consistency between the exact dynamics (defined by the ODE) and the approximating polynomials at the collocation points. They correspond to the error between the slope of the polynomials and the slope given by the ODE at the collocation nodes (see the first node of Fig. 2). Thus, the optimization problem results in a large-scale sparse NLP problem. For more details about pseudo-spectral control, one may consult [23].

Let us denote by $\boldsymbol{\mathcal{X}}_k(t_k, \tilde{\mathbf{x}}_k)$ and $\boldsymbol{\mathcal{W}}_k(t_k, \tilde{\mathbf{w}}_k)$ the piece-wise polynomial approximations of the state vector $\mathbf{x}(t)$ in the kth interval of discretization on a total of M segments, with $\tilde{\mathbf{x}}_k, \tilde{\mathbf{w}}_k$ the polynomial coefficients. The pseudo-spectral collocation may be formulated as follows:

$$\min \quad J\left(\tilde{\mathbf{x}}_k, \tilde{\mathbf{w}}_k\right) \tag{6a}$$

$$\text{w.r.t.} \quad \tilde{\mathbf{x}}_{k=1,\dots,M}, \tilde{\mathbf{w}}_{k=1,\dots,M}$$

$$\text{s.t.} \quad \dot{\boldsymbol{\mathcal{X}}}_k(t_k, \tilde{\mathbf{x}}_k) = f_{\text{ode}}\left(\boldsymbol{\mathcal{X}}_k(t_k, \tilde{\mathbf{x}}_k), \boldsymbol{\mathcal{W}}_k(t_k, \tilde{\mathbf{w}}_k)\right) \;\; k = 1, \dots, M-1 \tag{6b}$$

$$\mathbf{g}_{\text{path}}\left(\boldsymbol{\mathcal{X}}_k(t_k, \tilde{\mathbf{x}}_k), \boldsymbol{\mathcal{W}}_k(t_k, \tilde{\mathbf{w}}_k)\right) \leq 0 \tag{6c}$$

$$\boldsymbol{\mathcal{X}}_{k+1}(t_k, \tilde{\mathbf{x}}_{k+1}) - \boldsymbol{\mathcal{X}}_k(t_k, \tilde{\mathbf{x}}_k) = 0, \; k = 1, \dots, M-1 \tag{6d}$$

$$\mathbf{x_{min}} \leq \boldsymbol{\mathcal{X}}_k(t_k, \tilde{\mathbf{x}}_k) \leq \mathbf{x_{max}} \quad \forall t_k \in \mathcal{T} \tag{6e}$$

$$\mathbf{w_{min}} \leq \boldsymbol{\mathcal{W}}_k(t_k, \tilde{\mathbf{w}}_k) \leq \mathbf{w_{max}} \quad \forall t_k \in \mathcal{T} \tag{6f}$$

$$\mathbf{x}(t_0) = \mathbf{x}_0 \tag{6g}$$

$$\mathbf{x}(t_f) = \mathbf{x}_f \tag{6h}$$

Compared to single shooting techniques, the physical relevance of the trajectory is only ensured at the convergence of the optimal control problem since during optimization, the defect constraints could be violated or the initial node of segment kth and the last node of segment $k-1$th may not match. Because of the discretization of the state variables and control variables into segments, the gradient estimations are less sensitive to small perturbation of the control law parameters. Therefore, gradient-based algorithms may be used to solve such high-dimensional NLP problems with a large number of constraints. The introduction of such optimal control problem within a MDO problem rises different challenges and various MDO problem decompositions may be employed and are discussed in the next sections.

3. Multidisciplinary design optimization methods for launch vehicle analysis and optimization

3.1. Formulations for multidisciplinary optimal design of launch vehicles

Designing a launch vehicle is a multidisciplinary problem that requires to integrate all the necessary disciplines (*e.g.,* aerodynamics, propulsion, trajectory, structure) into a single process. In particular, these disciplines share a set of information, called *coupling variables* that have to be controlled by the design process in order for the optimal solution to be feasible. The optimization problem that results from the mathematical transcription of the MDO problem can be formulated as follows [6]:

$$\min \; f(\mathbf{z}, \mathbf{y}) \tag{7a}$$

$$\text{w.r.t.} \; \mathbf{z}, \mathbf{y}$$

$$\text{s.t.} \; \mathbf{g}(\mathbf{z}, \mathbf{y}) \leq 0 \tag{7b}$$

$$\mathbf{h}(\mathbf{z}, \mathbf{y}) = 0 \tag{7c}$$

$$\mathbf{y}_{ij} = \mathbf{c}_{ij}(\mathbf{z}, \mathbf{y}_{.i}), \forall (i,j) \in \{1, \dots, N\}^2, i \neq j \tag{7d}$$

$$\mathbf{z}_{\min} \leq \mathbf{z} \leq \mathbf{z}_{\max} \tag{7e}$$

$$\mathbf{y}_{\min} \leq \mathbf{y} \leq \mathbf{y}_{\max} \tag{7f}$$

with:

- $f(\cdot)$: the objective function to be optimized (*e.g.*, Gross-Lift-Off-Weight),
- $\mathbf{z}$: the architectural design variable vector $\mathbf{z} \in \mathbb{R}^p$ (*e.g.*, propellant masses, launch vehicle stage diameters, combustion chamber pressure),
- $\mathbf{y}$: the coupling vector that is composed of the variables that traduce the interactions between the disciplines and constitute the inputs of the different disciplines (*e.g.*, dry mass for trajectory, axial load factor for structure)
- $\mathbf{g}(\cdot)$: the vector of inequality constraint functions (*e.g.*, axial and transverse maximum load factors, maximum dynamic pressure),
- $\mathbf{h}(\cdot)$: the vector of equality constraint functions (*e.g.*, target orbit altitude and velocity),
- $\mathbf{c}(\cdot)$: the coupling responses of the disciplines, that are the outputs of the different disciplines (*e.g.*, aerodynamic coefficients for aerodynamics, thrust for propulsion).

and N the number of disciplines. The main particularity of MDO problems is the handling of interdisciplinary coupling satisfaction inside the design process (Eq. (8)). In a two disciplines context (Fig. 3), the couplings between the disciplines i and j are said to be *satisfied* when the following interdisciplinary system of non-linear equations is verified:

$$\forall (i,j) \in \{1, \dots, N\}^2, i \neq j, \; \begin{cases} \mathbf{y}_{ij} = \mathbf{c}_{ij}(\mathbf{z}_i, \mathbf{y}_{.i}) \\ \mathbf{y}_{ji} = \mathbf{c}_{ji}(\mathbf{z}_j, \mathbf{y}_{.j}) \end{cases} \tag{8}$$

with $\mathbf{y}_{ji}$ the input coupling vector in discipline i coming from discipline j, $\mathbf{z}_i$ the subset of the design variable vector $\mathbf{z}$ that inputs discipline $c_{i.}(\cdot)$,

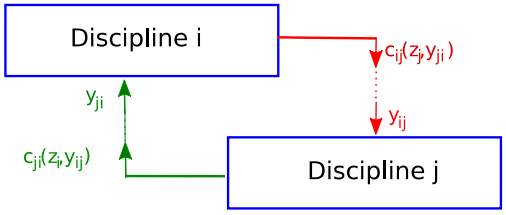

Fig. 3. Input and output coupling variables inside an MDO process.

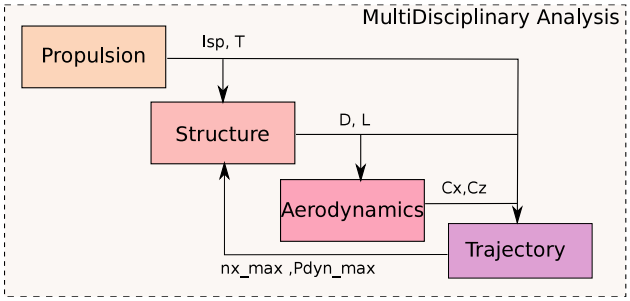

Fig. 4. Typical interactions between the main disciplines involved into a launch vehicle design process, with: Isp the specific impulse ; T the thrust ; D the diameter of the vehicle ; L the length of the vehicle ; Cx and Cz the drag and lift coefficients ; nx_{max} the maximal load factor and $Pdyn_{max}$ the maximal dynamic pressure.

$\mathbf{y}_{.i}$ the subset of the input coupling vector $\mathbf{y}$ that enters discipline $c_{i.}(\cdot)$ and N the number of disciplines.

Example of coupled design process used at the early design of launch vehicle is given in Fig. 4.

Regarding the optimal control problem described in Section 2, this MDO problem formulation can be extended to include trajectory optimization as follows:

$$\min \ f(\mathbf{z}, \mathbf{y}, \mathbf{w}(t)) \tag{9a}$$
$$\text{w.r.t. } \mathbf{z}, \mathbf{y}, \mathbf{w}(t)$$
$$\text{s.t. } \mathbf{g}(\mathbf{z}, \mathbf{y}) \leq 0 \tag{9b}$$
$$\mathbf{h}(\mathbf{z}, \mathbf{y}) = 0 \tag{9c}$$
$$\mathbf{y}_{ij} = \mathbf{c}_{ij}(\mathbf{z}, \mathbf{y}_{.i}), \forall (i,j) \in \{1, \dots, N\}^2, i \neq j \tag{9d}$$
$$\dot{\mathbf{x}}(t) = f_{\text{ode}}(\mathbf{z}, \mathbf{y}, \mathbf{x}(t), \mathbf{w}(t)) \tag{9e}$$
$$\mathbf{g}_{\text{path}}(\mathbf{z}, \mathbf{y}, \mathbf{x}(t), \mathbf{w}(t)) \leq 0 \tag{9f}$$
$$\mathbf{x_{min}} \leq \mathbf{x}(t) \leq \mathbf{x_{max}} \quad \forall t \in \mathcal{T} \tag{9g}$$
$$\mathbf{w_{min}} \leq \mathbf{w}(t) \leq \mathbf{w_{max}} \quad \forall t \in \mathcal{T} \tag{9h}$$
$$\mathbf{x}(t_0) = \mathbf{x}_0 \tag{9i}$$
$$\mathbf{x}(t_f) = \mathbf{x}_f \tag{9j}$$
$$\mathbf{z}_{\min} \leq \mathbf{z} \leq \mathbf{z}_{\max} \tag{9k}$$
$$\mathbf{y}_{\min} \leq \mathbf{y} \leq \mathbf{y}_{\max} \tag{9l}$$

In that case, the optimization criterion for trajectory $J(\cdot)$ can be included either in the objective function $f(\cdot)$ or in the design constraint $g(\cdot)$ without loss of generality. Different approaches that combine the MDO problem formulation and the optimal control problem solving can be proposed. The main existing approaches are reviewed in the following section.

3.2. Coupled MDO formulation for launch vehicle design

The main coupled MDO formulation, called MultiDiscipline Feasible (MDF) formulation [8,24] is the most used MDO method to solve the launch vehicle design problem [6]. In this formulation, the interdisciplinary coupling consistency is ensured using a MultiDisciplinary Analysis (MDA). MDA ensures multidisciplinary feasibility, meaning that the MDO optimal solution has to satisfy the interdisciplinary couplings between the input coupling variable vector $\mathbf{y}$ and the output coupling variable vector, which is the output of the coupling functions gathered in $\mathbf{c}(\cdot)$ resulting from the discipline simulations. Typically, MDA can be solved using fixed point iteration (*e.g.*, Gauss Seidel algorithm) between the different disciplines.

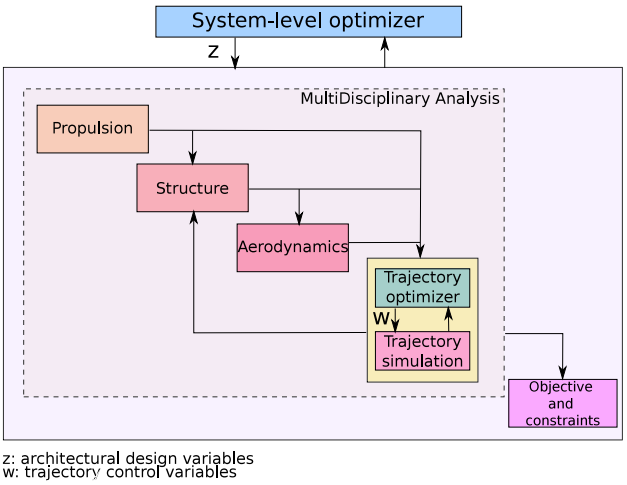

Fig. 5. MDF with nested trajectory optimization formulation and MultiDisciplinary Analysis.

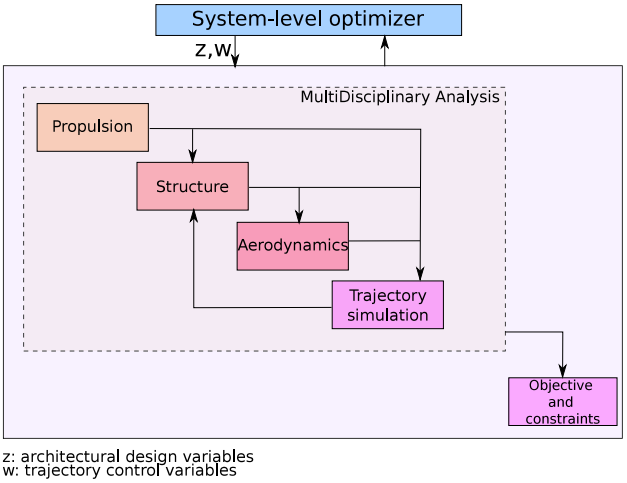

Fig. 6. MDF with nested trajectory simulation formulation and MultiDisciplinary Analysis.

Considering the optimal control problem, it can be solved in different manners in an MDF formulation. Either the optimal control is handled inside the trajectory discipline, in that case, the system optimizer only controls the design variables (Fig. 5), or the optimal control variables are handled at the same level as the design variables by the optimizer (Fig. 6). In the first case, two optimization problems are nested (optimization of trajectory inside the optimization of the launch vehicle design), whereas in the second case, only one optimization is performed on an augmented space (design and control law variables).

At the system-level, the optimization problem in the MDF with nested trajectory optimization can be formulated as follows:

$$\min \ f(\mathbf{z}, \mathbf{y}(\mathbf{z})) \tag{10a}$$
$$\text{w.r.t. } \mathbf{z}$$
$$\text{s.t. } \mathbf{g}(\mathbf{z}, \mathbf{y}(\mathbf{z})) \leq 0 \tag{10b}$$

$$\mathbf{h}(\mathbf{z}, \mathbf{y}(\mathbf{z})) = 0 \tag{10c}$$

$$\mathbf{z}_{\min} \leq \mathbf{z} \leq \mathbf{z}_{\max} \tag{10d}$$

In that case, the optimizer only controls the design variables $\mathbf{z}$. The coupling variables $\mathbf{y}$ are handled by the MDA and the control variables $\mathbf{w}(t)$ are directly handled inside the trajectory discipline.

In the second formulation, *i.e.* MDF with nested trajectory simulation, considering here the direct single shooting technique for the sake of simplicity, the optimization at the system level can be written as:

$$\min \ f(\mathbf{z}, \mathbf{y}(\mathbf{z}, \mathbf{w}(t)), \mathbf{w}(t)) \tag{11a}$$

$$\text{w.r.t. } \mathbf{z}, \mathbf{w}(t)$$

$$\text{s.t. } \mathbf{g}(\mathbf{z}, \mathbf{y}(\mathbf{z}, \mathbf{w}(t))) \leq 0 \tag{11b}$$

$$\mathbf{h}(\mathbf{z}, \mathbf{y}(\mathbf{z}, \mathbf{w}(t))) = 0 \tag{11c}$$

$$\mathbf{g}_{\text{path}}(\mathbf{z}, \mathbf{y}(\mathbf{z}, \mathbf{w}(t)), \mathbf{x}(t), \mathbf{w}(t)) \leq 0 \tag{11d}$$

$$\mathbf{x}_{t_f}(\mathbf{z}, \mathbf{y}(\mathbf{z}, \mathbf{w}(t)), \mathbf{w}(t)) = \mathbf{x}_f \tag{11e}$$

$$\mathbf{z}_{\min} \leq \mathbf{z} \leq \mathbf{z}_{\max} \tag{11f}$$

$$\mathbf{w}_{\min} \leq \mathbf{w}(t) \leq \mathbf{w}_{\max} \quad \forall t \in \mathcal{T} \tag{11g}$$

In case pseudo-spectral technique for optimal control is used, the discretized values of the state variables $\mathbf{x}$ are also handled as optimization variables.

In the MDF with nested trajectory optimization formulation (Fig. 5) [25–28], at each iteration of the system-level optimizer and at each iteration of the MDA solving Eq. (8), the trajectory discipline carries out an analysis consisting in solving the optimal control problem Eqs. (1b)–(1g). The system-level optimizer only controls the architectural design variables $\mathbf{z}$. It results in a nested triple loop process (outer loop: MDF, middle loop: MDA and inner loop: optimal control) leading to a large computational cost especially when high fidelity models (*e.g.*, Computational Fluid Dynamics, Finite Element Method) are used. At each iteration of the MDA, the output coupling variables of the trajectory corresponds to the value for an optimal trajectory. In the MDF with nested trajectory simulation formulation (Fig. 6) [29–32], the loop corresponding to the trajectory optimization is removed and only trajectory simulation is carried out inside the MDA. The system-level optimizer is in charge to control both the architectural design variables $\mathbf{z}$ and the trajectory control variables $\mathbf{w}$, and to satisfy the path constraints related to the trajectory.

This results in a nested double loop process (outer loop: MDF, inner loop: MDA). At each iteration of the MDA, the output coupling variables of the trajectory correspond to the results of the trajectory simulation given the current trajectory control variable values given by the system-level optimizer. In general, compared to MDF with nested trajectory optimization formulation, MDF with nested trajectory simulation formulation reduces the associated computational cost. However, due to the presence of MDA, it still involves a high number of discipline evaluations.

3.3. Decoupled formulation for launch vehicle design

In order to break the nested loops and to avoid MDA, decoupled formulations have been introduced [8,33] and used for launch vehicle design in a limited number of papers [34–38]. The general idea of decoupled formulations is to introduce additional optimization variables such as the input coupling variables $\mathbf{y}$ and additional constraints such as interdisciplinary coupling constraints (see Eq. (12d)). Therefore, all the optimization variables are controlled at the system-level (the architectural design variables $\mathbf{z}$, the input coupling variables $\mathbf{y}$). The multidisciplinary feasibility is only ensured at the system-level optimizer convergence whereas with MDF approach it is ensured at each iteration of the system-level optimizer. Different decoupled approaches have been proposed, the most known are Individual Discipline Feasible (IDF) and All-At-Once (AAO) [8]. The main difference between these two formulations is the handling of disciplinary local variables (also sometimes referred as state variables). These variables are related to the satisfaction of a state equation internal to the discipline and in general represents an equilibrium state (for instance thermo-chemical equilibrium in engine combustion). In IDF, these variables are handle inside the different disciplines (which are called discipline analyzers) whereas in AAO, the local variables are handled as the optimization variables along with the design variables by the system level optimizer [6] and the disciplines are called discipline evaluators.

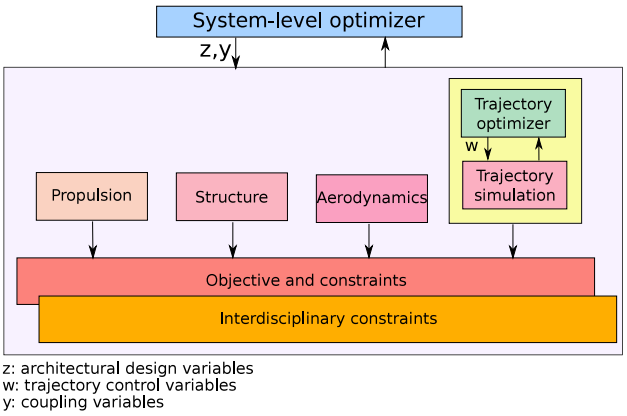

Fig. 7. IDF formulation for launch vehicle design.

Regarding the handling of trajectory optimization inside the MDO formulation, both IDF and AAO can be used. Indeed, in the case where the trajectory discipline is responsible for the trajectory optimization, an IDF formulation of the MDO problem can be proposed as follows:

$$\min \ f(\mathbf{z}, \mathbf{y}) \tag{12a}$$

$$\text{w.r.t } \mathbf{z}, \mathbf{y}$$

$$\text{s.t. } \mathbf{g}(\mathbf{z}, \mathbf{y}) \leq 0 \tag{12b}$$

$$\mathbf{h}(\mathbf{z}, \mathbf{y}) = 0 \tag{12c}$$

$$\mathbf{y}_{ij} = \mathbf{c}_{ij}(\mathbf{z}, \mathbf{y}_{.i}), \forall (i,j) \in \{1, \ldots, N\}^2, i \neq j \tag{12d}$$

$$\mathbf{g}_{\text{path}}(\mathbf{z}, \mathbf{y}, \mathbf{x}(t), \mathbf{w}(t)) \leq 0 \tag{12e}$$

$$\mathbf{z}_{\min} \leq \mathbf{z} \leq \mathbf{z}_{\max} \tag{12f}$$

$$\mathbf{y}_{\min} \leq \mathbf{y} \leq \mathbf{y}_{\max} \tag{12g}$$

In this case, the control law $\mathbf{w}(t)$ is handled inside the trajectory discipline and these variables do not appear in the system level optimization problem (Fig. 7).

In the case the system level optimizer handles both the design and control variables in a decoupled formulation, the AAO formulation can be used. In this case, the trajectory discipline only evaluates the system of equations of motion. The system level optimizer handles the design variables $\mathbf{z}$, the interdisciplinary coupling variables $\mathbf{y}$ and the control law $\mathbf{w}(t)$. In this case, the coupling constraints and trajectory path constraints are also added to the system level optimization problem to ensure, at the convergence of the optimization process, the coupling consistency and the trajectory consistency. The AAO formulation of the launch vehicle design problem (Fig. 8) may be expressed as:

$$\min \ f(\mathbf{z}, \mathbf{y}, \mathbf{w}(t)) \tag{13a}$$

$$\text{w.r.t. } \mathbf{z}, \mathbf{y}, \mathbf{w}(t)$$

$$\text{s.t. } \mathbf{g}(\mathbf{z}, \mathbf{y}, \mathbf{w}(t)) \leq 0 \tag{13b}$$

$$\mathbf{h}(\mathbf{z}, \mathbf{y}, \mathbf{w}(t)) = 0 \tag{13c}$$

$$\mathbf{g}_{\text{path}}(\mathbf{z}, \mathbf{y}, \mathbf{w}(t)) \leq 0 \tag{13d}$$

$$\mathbf{y}_{ij} = \mathbf{c}_{ij}(\mathbf{z}, \mathbf{y}_{.i}, \mathbf{w}(t)), \forall (i,j) \in \{1, \ldots, N\}^2, i \neq j \tag{13e}$$

$$\mathbf{x}_{t_f}(\mathbf{z}, \mathbf{y}(\mathbf{z}, \mathbf{w}(t)), \mathbf{w}(t)) = \mathbf{x}_f \tag{13f}$$

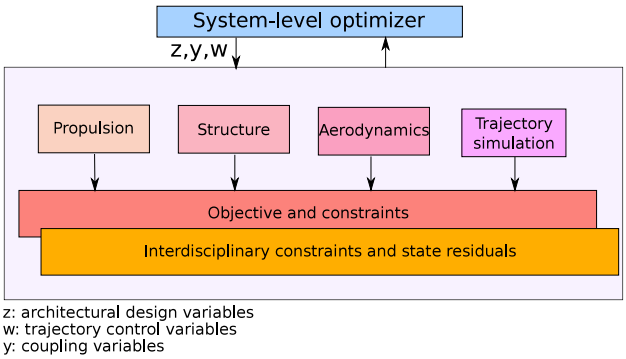

Fig. 8. AAO formulation for launch vehicle design.

$$\mathbf{w_{min}} \leq \mathbf{w}(t) \leq \mathbf{w_{max}} \quad \forall t \in \mathcal{T} \tag{13g}$$

$$\mathbf{z}_{\min} \leq \mathbf{z} \leq \mathbf{z}_{\max} \tag{13h}$$

Compared to MDF, in the decoupled MDO formulations, the system level optimizer controls $\mathbf{z}, \mathbf{y}$, and an additional constraint is added to ensure multidisciplinary feasibility at the convergence of the optimization problem. The main difference between these two formulations is about the handling of trajectory variables which is performed inside the trajectory in the IDF formulation and at the system-level in the AAO formulation.

AAO formulation of the problem allows to avoid the MDA loops and combine the optimal control problem for the trajectory with the system-level optimization problem removing all the nested loops. However, it increases the number of optimization variables that has to be controlled at the system-level and it increases the number of equality constraints causing a more difficult optimization problem to be solved.

MDF, IDF and AAO are very generic formulations and do not specify the type of optimal control inside the trajectory. As explained above, the trajectory discipline is a key module and different approaches exist to transcript the optimal control problem into an optimization problem. In the next Section, the proposed MDO formulation, coupling AAO and pseudo-spectral method for trajectory, is described.

4. Approach combining of AAO with pseudo-spectral method for launch vehicle analysis and optimization

4.1. Proposed MDO formulation of the launch vehicle design optimization

The proposed MDO formulation which is referred to as the All-At-Once Pseudo-Spectral (AAO-PS) formulation for launch vehicle design. It combines the All-At-Once (AAO) formulation and the pseudo-spectral method for the trajectory solving (Fig. 9). Compared to the traditional approach (MDF), the proposed formulation avoids the three layers nested loop (system-level optimizer, MDA and trajectory optimizer) in order to reduce the computational cost. Moreover, the proposed approach exploits the commonalities of AAO and pseudo-spectral techniques: both decouple the optimization problem in order to efficiently solve it by considering additional optimization variables and additional optimization constraints. Indeed, AAO formulations add the input interdisciplinary couplings and the states variables as optimization variables controlled at the system-level along with the architectural design variables. In the pseudo-spectral techniques, the state variables and the control variables approximated as piece-wise polynomials are controlled by the optimizer. Moreover, in AAO additional interdisciplinary constraints and residuals for the state variables are added in the formulation and in the pseudo-spectral technique defect constraints and matching of discretization nodes are also added. The feasibility of the launch vehicle design and its trajectory is ensured only at the optimization convergence. Indeed, AAO ensures the interdisciplinary coupling satisfaction at the convergence of the MDO problem solving and pseudo-spectral technique ensures the trajectory feasibility through physical relevance only at the convergence of the optimal control problem. In the following, to ease the notation, $\tilde{\mathbf{x}} = \tilde{\mathbf{x}}_{k=1,\dots,M}$ and $\tilde{\mathbf{w}} = \tilde{\mathbf{w}}_{k=1,\dots,M}$. The proposed AAO-formulation with pseudo-spectral approach for launch vehicle design is expressed as:

$$\min \; f(\mathbf{z}, \mathbf{y}, \tilde{\mathbf{x}}, \tilde{\mathbf{w}}) \tag{14a}$$

$$\text{w.r.t. } \mathbf{z}, \mathbf{y}, \tilde{\mathbf{x}}, \tilde{\mathbf{w}}$$

$$\text{s.t. } \mathbf{g}(\mathbf{z}, \mathbf{y}, \tilde{\mathbf{x}}, \tilde{\mathbf{w}}) \leq 0 \tag{14b}$$

$$\mathbf{h}(\mathbf{z}, \mathbf{y}, \tilde{\mathbf{x}}, \tilde{\mathbf{w}})) = 0 \tag{14c}$$

$$\mathbf{y}_{ij} = \mathbf{c}_{ij}(\mathbf{z}, \mathbf{y}_{.i}, \tilde{\mathbf{x}}, \tilde{\mathbf{w}}), \forall (i,j) \in \{1, \dots, N\}^2, i \neq j \tag{14d}$$

$$\dot{\mathcal{X}}_k(t_k, \tilde{\mathbf{x}}_k) = f_{\text{ode}}\left(\mathbf{z}, \mathbf{y}, \mathcal{X}_k(t_k, \tilde{\mathbf{x}}_k), \mathcal{W}_k(t_k, \tilde{\mathbf{w}}_k)\right) \; k = 1, \dots, M-1 \tag{14e}$$

$$\mathbf{g}_{\text{path}}\left(\mathbf{z}, \mathbf{y}(\mathbf{z}), \mathcal{X}(t, \tilde{\mathbf{x}}), \mathcal{W}(t, \tilde{\mathbf{w}})\right) \leq 0 \tag{14f}$$

$$\mathcal{X}_{k+1}(t_k, \tilde{\mathbf{x}}_{k+1}) - \mathcal{X}_k(t_k, \tilde{\mathbf{x}}_k) = 0, \; k = 1, \dots, M-1 \tag{14g}$$

$$\mathbf{x_{min}} \leq \mathcal{X}(t, \tilde{\mathbf{x}}) \leq \mathbf{x_{max}} \quad \forall t \in \mathcal{T} \tag{14h}$$

$$\mathbf{w_{min}} \leq \mathcal{W}(t, \tilde{\mathbf{w}}) \leq \mathbf{w_{max}} \quad \forall t \in \mathcal{T} \tag{14i}$$

$$\mathbf{x}(t_0) = \mathbf{x}_0 \tag{14j}$$

$$\mathbf{x}(t_f) = \mathbf{x}_f \tag{14k}$$

$$\mathbf{z}_{\min} \leq \mathbf{z} \leq \mathbf{z}_{\max} \tag{14l}$$

In the proposed approach, the whole MDO of the launch vehicle is driven by a single optimizer at the system-level. It controls the architectural design variables $\mathbf{z}$, the input coupling variables $\mathbf{y}$, the states and control variables nodes for the trajectory $\tilde{\mathbf{x}}_{k=1,\dots,M}, \tilde{\mathbf{w}}_{k=1,\dots,M}$. Depending on the polynomial choice and the number of democratization nodes, the number of optimization variables and the number of equality constraints vary between few hundreds and few thousands and therefore only gradient-based techniques are able to efficiently solve such a complex optimization problem.

Therefore, a key element is to estimate the gradients for the MDO objective function and constraints including all the quantity of interests in the trajectory simulation at an affordable computational cost. It is critical that the gradient calculation does not introduce numerical noise to ensure optimization convergence. In the implementation of the proposed MDO formulation, the DYMOS package [39] of the OpenMDAO framework [40] is used. OpenMDAO is a MDO framework allowing efficient total derivatives calculation and Dymos is its optimal control library. Considering that the analytical partial derivatives of the disciplinary output vector with respect to the disciplinary input vector are provided, DYMOS relies on the ability of OpenMDAO to compute total derivatives efficiently using chain rule and the partial derivatives. It allows to compute gradients analytically and propagate the derivatives in the whole MDO process including through the trajectory discipline. Therefore, it facilitates the use of gradient-based optimizer to solve MDO problem which includes an optimal control problem.

4.2. Derivation of the MDO formulation for uncertainty quantification

In early design phases, due to modeling simplifications, numerical approximations and environmental uncertainties, a large number of uncertain parameters should be considered especially in MDO process which involves different physics and disciplines, for instance, uncertainties related to the specific impulse, the mass flow rate, the structural mass, the nozzle geometry, ODE solver accuracy, *etc.* In order to limit the computational cost associated to uncertainty quantification (UQ) studies, Sensitivity Analysis (SA) may be used to provide an overview of the behavior of the system under uncertainty by ranking the uncertainty variables by importance on a quantity of interest. Therefore, considering a vector of uncertain parameters $\mathbf{U} = [U_1, \dots, U_d]$ of dimension d defined according to a Probability Density Function (PDF) $\phi(\mathbf{U})$, the purpose of SA is to determine the influence of the input

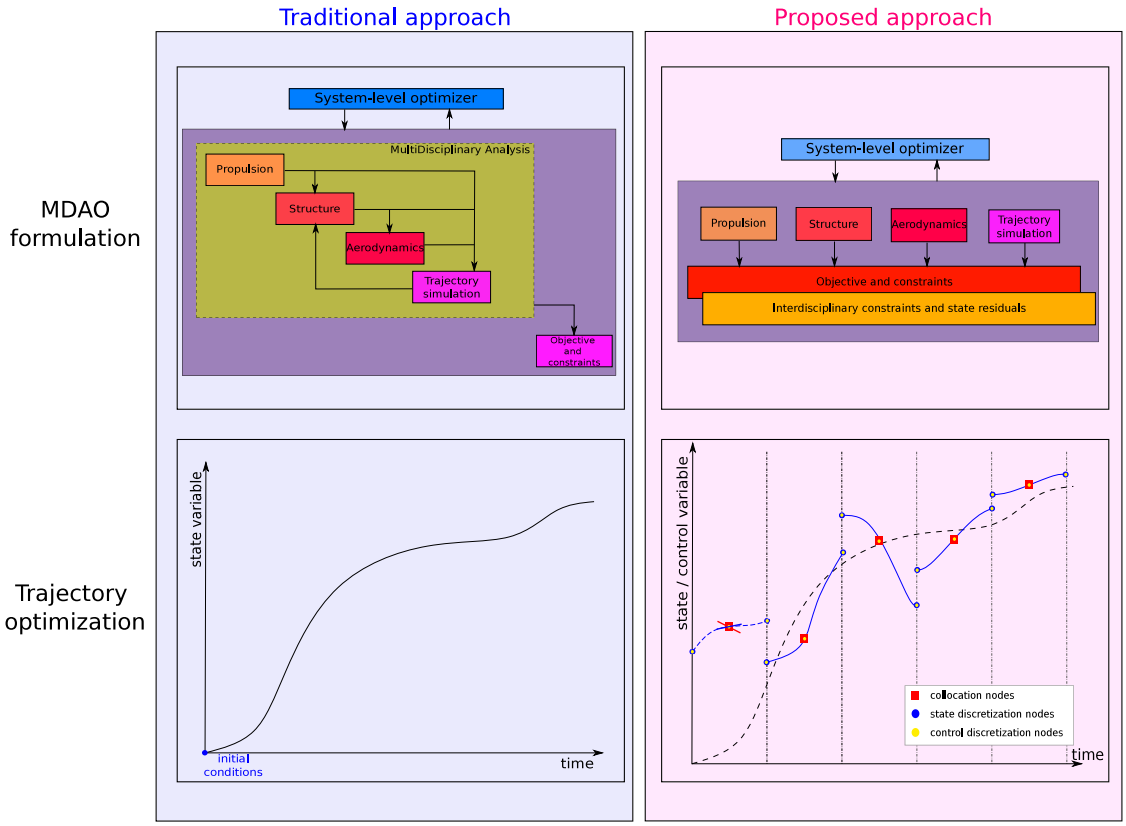

Fig. 9. Traditional (MDF) and proposed MDO formulation for launch vehicle design based on All-At-Once and pseudo-spectral technique.

variables $\mathbf{U}$ on a quantity of interest $Y = f(\mathbf{U})$ with $f(\cdot)$ a model. With SA, it is for instance possible to identify the variables with almost no influence on system performance (or constraints) and to freeze them to nominal values, reducing the dimensionality for UQ studies. Different SA techniques may be used depending on the analysis purpose such as Morris technique [13], Sobol' indices [14], HSIC indices [15]. In the context of MDAO process with an access to analytic gradient (as discussed in the previous section), the Derivative-based Global Sensitivity Measures (DGSM) is an interesting sensitivity method [17]. DGSM is a global (over the entire definition domain of the uncertain variables) SA approach that generally requires fewer function evaluations than the Sobol' indices [16,41], provided that the partial derivatives of the quantity of interest are available. For more details about sensitivity analysis, one may consult [16]. The first order DGSM index corresponding to variable U_i can be defined as:

$$v_i^{(1)} = \int_{\mathbb{R}^d} \frac{\mathrm{d}f}{\mathrm{d}u_i}(\mathbf{u})\phi(\mathbf{u})\mathrm{d}\mathbf{u} \tag{15}$$

where $\phi(\cdot)$ is the joint PDF of the uncertain vector $\mathbf{U}$. The second order DGSM index is defined as follows:

$$v_i^{(2)} = \int_{\mathbb{R}^d} \left(\frac{\mathrm{d}f}{\mathrm{d}u_i}(\mathbf{u})\right)^2 \phi(\mathbf{u})\mathrm{d}\mathbf{u} \tag{16}$$

These sensitivity indices use the derivatives of the quantity of interest with respect to the uncertainty and perform an integral of this quantity with respect to the PDF of the uncertainty parameters. DGSM have been widely used for identifying the most influential variables and links with Sobol' indices have been made in Kucherenko and Song [17]. This kind of indices is particularly interesting in case of design processes providing derivatives because it allows to perform a sensitivity analysis at a reduced computational cost. Let us consider a generic AAO problem (without all the pseudo-spectral part to simplify the notations but without loss of generality) with a realization $\mathbf{u}_0$ of an uncertain variable vector $\mathbf{U}$ sampled according to $\phi(\cdot)$:

$$\begin{aligned}
&\min\ f(\boldsymbol{\zeta}, \mathbf{u}_0) && \text{(17a)}\\
&\text{w.r.t. } \boldsymbol{\zeta} &&\\
&\text{s.t. } \mathbf{g}(\boldsymbol{\zeta}, \mathbf{u}_0) \le 0 && \text{(17b)}\\
&\quad \mathbf{h}(\boldsymbol{\zeta}, \mathbf{u}_0) = 0 && \text{(17c)}\\
&\quad \mathbf{c}(\boldsymbol{\zeta}, \mathbf{u}_0) = 0 && \text{(17d)}\\
&\quad \boldsymbol{\zeta}_{\min} \le \boldsymbol{\zeta} \le \boldsymbol{\zeta}_{\max} && \text{(17e)}
\end{aligned}$$

with $\boldsymbol{\zeta} = \{\mathbf{z}, \mathbf{y}, \mathbf{w}(t)\}$ and $\mathbf{c}(\boldsymbol{\zeta}, \mathbf{u}_0) = 0$ corresponding to the interdisciplinary constraints rewritten as $\mathbf{y}_{ij} - \mathbf{c}_{ij}(\mathbf{z}, \mathbf{y}_{,i}, \mathbf{w}(t), \mathbf{u}_0) = 0, \forall (i,j) \in \{1,\dots,N\}^2, i \neq j$ to simplify the following derivations. The MDO problem is solved for a particular realization of the uncertain variable vector. However, considering another realization of the uncertain variable vector will lead to a different optimal solution and therefore a different performance at the optimum. In this context, the purpose of the SA is to characterize the impact of the uncertain variables vector $\mathbf{U}$ on the objective function $f(\cdot)$ at the optimum of the MDO problem. Therefore, it provides an indication of the influence of the uncertain parameters on the performance of the launch vehicle. To efficiently compute the DGSM indices, post-optimality analysis after MDO problem solving for a particular realization of the uncertain variables may be used to compute the gradient of the objective function with respect to a local variation of the uncertain variable vector without having to re-optimize the launch vehicle for this variation. This technique allows to estimate the gradient of the objective function $f(\cdot)$ from the Lagrange multipliers associated to the 1st order Karush–Kuhn–Tucker (KKT) conditions [42]. It avoids to estimate the gradient using finite differences and therefore re-optimizations of the launch vehicle for each local variation of the uncertain variable vector. The post-optimality analysis consists in efficiently computing:

$$\frac{\mathrm{d}f}{\mathrm{d}u_q}(\boldsymbol{\zeta}^*, \mathbf{u}) = \frac{\partial f}{\partial u_q}(\boldsymbol{\zeta}^*, \mathbf{u}) + \frac{\partial f}{\partial \boldsymbol{\zeta}}\frac{\partial \boldsymbol{\zeta}}{\partial u_q}(\boldsymbol{\zeta}^*, \mathbf{u}) \tag{18}$$

with $\boldsymbol{\zeta}^*$ the optimal solution of the optimization problem Eqs. (14)–(14l). Post-optimality analysis has been applied in different aerospace vehicle design problems [18,43,44]. The novelty here is to combine global SA technique based on DGSM indices and post-optimality analysis in order to provide valuable information on the sensitivity of the optimal launch vehicle performance with respect to uncertainty in early design phases at an affordable computational cost.

Considering the first order KKT to the proposed AAO-PS formulation, then:

$$\frac{\partial f}{\partial \boldsymbol{\zeta}}(\boldsymbol{\zeta}^*,\mathbf{u}) + \sum_{i=1}^{n_h} \lambda_i \frac{\partial h_i}{\partial \boldsymbol{\zeta}}(\boldsymbol{\zeta}^*,\mathbf{u}) + \sum_{j=1}^{n_g} \mu_j \frac{\partial g_j}{\partial \boldsymbol{\zeta}}(\boldsymbol{\zeta}^*,\mathbf{u}) + \sum_{k=1}^{n_c} \eta_k \frac{\partial c_k}{\partial \boldsymbol{\zeta}}(\boldsymbol{\zeta}^*,\mathbf{u}) = 0 \tag{19a}$$

$$\mathbf{h}(\boldsymbol{\zeta}^*,\mathbf{u}) = 0 \tag{19b}$$

$$\mathbf{g}(\boldsymbol{\zeta}^*,\mathbf{u}) \leq 0 \tag{19c}$$

$$\mathbf{c}(\boldsymbol{\zeta}^*,\mathbf{u}) = 0 \tag{19d}$$

$$\lambda_i \geq 0 \text{ for } i \in [1, n_h] \tag{19e}$$

$$\mu_j \geq 0 \text{ for } j \in [1, n_g] \tag{19f}$$

$$\eta_k \geq 0 \text{ for } k \in [1, n_c] \tag{19g}$$

$$\lambda_i h_i(\boldsymbol{\zeta}^*,\mathbf{u}) = 0 \text{ for } i \in [1, n_h] \tag{19h}$$

$$\mu_j g_j(\boldsymbol{\zeta}^*,\mathbf{u}) = 0 \text{ for } j \in [1, n_g] \tag{19i}$$

$$\eta_k c_k(\boldsymbol{\zeta}^*,\mathbf{u}) = 0 \text{ for } k \in [1, n_c] \tag{19j}$$

with λ, $\boldsymbol{\mu}$ and $\boldsymbol{\eta}$ the different Lagrange multipliers. In the following, only the saturated inequality constraints are considered (as $\mu_j = 0$ for a non saturated inequality constraint $g_j(\cdot)$). Assuming that the set of saturated inequality constraints stays saturated under a small variation of $\mathbf{u}$. Then,

$$\frac{dh_i}{du_q}(\boldsymbol{\zeta}^*,\mathbf{u}) = \frac{\partial h_i}{\partial u_q}(\boldsymbol{\zeta}^*,\mathbf{u}) + \frac{\partial h_i}{\partial \boldsymbol{\zeta}}\frac{\partial \boldsymbol{\zeta}}{\partial u_q}(\boldsymbol{\zeta}^*,\mathbf{u}) = 0 \rightarrow \frac{\partial h_i}{\partial \boldsymbol{\zeta}}\frac{\partial \boldsymbol{\zeta}}{\partial u_q}(\boldsymbol{\zeta}^*,\mathbf{u}) = -\frac{\partial h_i}{\partial u_q}(\boldsymbol{\zeta}^*,\mathbf{u}) \tag{20a}$$

$$\frac{dg_j}{du_q}(\boldsymbol{\zeta}^*,\mathbf{u}) = \frac{\partial g_j}{\partial u_q}(\boldsymbol{\zeta}^*,\mathbf{u}) + \frac{\partial g_j}{\partial \boldsymbol{\zeta}}\frac{\partial \boldsymbol{\zeta}}{\partial u_q}(\boldsymbol{\zeta}^*,\mathbf{u}) = 0 \rightarrow \frac{\partial g_j}{\partial \boldsymbol{\zeta}}\frac{\partial \boldsymbol{\zeta}}{\partial u_q}(\boldsymbol{\zeta}^*,\mathbf{u}) = -\frac{\partial g_j}{\partial u_q}(\boldsymbol{\zeta}^*,\mathbf{u}) \tag{20b}$$

$$\frac{dc_k}{du_q}(\boldsymbol{\zeta}^*,\mathbf{u}) = \frac{\partial c_k}{\partial u_q}(\boldsymbol{\zeta}^*,\mathbf{u}) + \frac{\partial c_k}{\partial \boldsymbol{\zeta}}\frac{\partial \boldsymbol{\zeta}}{\partial u_q}(\boldsymbol{\zeta}^*,\mathbf{u}) = 0 \rightarrow \frac{\partial c_k}{\partial \boldsymbol{\zeta}}\frac{\partial \boldsymbol{\zeta}}{\partial u_q}(\boldsymbol{\zeta}^*,\mathbf{u}) = -\frac{\partial c_k}{\partial u_q}(\boldsymbol{\zeta}^*,\mathbf{u}) \tag{20c}$$

Moreover, with Eq. (19a):

$$\frac{\partial f}{\partial \boldsymbol{\zeta}}\frac{\partial \boldsymbol{\zeta}}{\partial u_q}(\boldsymbol{\zeta}^*,\mathbf{u}) + \sum_{i=1}^{n_h} \lambda_i \frac{\partial h_i}{\partial \boldsymbol{\zeta}}\frac{\partial \boldsymbol{\zeta}}{\partial u_q}(\boldsymbol{\zeta}^*,\mathbf{u}) + \sum_{j=1}^{n_g} \mu_j \frac{\partial g_j}{\partial \boldsymbol{\zeta}}\frac{\partial \boldsymbol{\zeta}}{\partial u_q}(\boldsymbol{\zeta}^*,\mathbf{u}) + \sum_{k=1}^{n_c} \eta_k \frac{\partial c_k}{\partial \boldsymbol{\zeta}}\frac{\partial \boldsymbol{\zeta}}{\partial u_q}(\boldsymbol{\zeta}^*,\mathbf{u}) = 0 \tag{21}$$

Then, by combining Eq. (21), Eqs. (20a)–(20c) and Eq. (18), it is possible to efficiently estimate the derivative of the objective function with respect to the uncertain variables:

$$\frac{\mathrm{d}f}{\mathrm{d}u_q}(\boldsymbol{\zeta}^*,\mathbf{u}) = \frac{\partial f}{\partial u_q}(\boldsymbol{\zeta}^*,\mathbf{u}) + \sum_{i=1}^{n_h} \lambda_i \frac{\partial h_i}{\partial u_q}(\boldsymbol{\zeta}^*,\mathbf{u}) + \sum_{j=1}^{n_g} \mu_j \frac{\partial g_j}{\partial u_q}(\boldsymbol{\zeta}^*,\mathbf{u}) + \sum_{k=1}^{n_c} \eta_k \frac{\partial c_k}{\partial u_q}(\boldsymbol{\zeta}^*,\mathbf{u}) \tag{22}$$

Finally, the DGSM index for the qth component of the uncertain variable vector can be computed as follows:

$$\upsilon_q^{(l)} = \int_{\mathbb{R}^d} \left(\frac{\partial f}{\partial u_q}(\boldsymbol{\zeta}^*,\mathbf{u}) + \sum_{i=1}^{n_h} \lambda_i \frac{\partial h_i}{\partial u_q}(\boldsymbol{\zeta}^*,\mathbf{u}) + \sum_{j=1}^{n_g} \mu_j \frac{\partial g_j}{\partial u_q}(\boldsymbol{\zeta}^*,\mathbf{u}) + \sum_{k=1}^{n_c} \eta_k \frac{\partial c_k}{\partial u_q}(\boldsymbol{\zeta}^*,\mathbf{u}) \right)^l \phi(\mathbf{u})\mathrm{d}\mathbf{u} \tag{23}$$

with l the order of the sensitivity index ($l = 1$ for the first order DGSM index and $l = 2$ for a second order DGSM index). Therefore, the post-optimality analysis allows to estimate the gradient of the system performance with respect to the uncertain variable vector by combining analytical partial derivatives of the objective function and analytical partial derivatives of the different active constraints with the optimal Lagrange multipliers. This allows to reduce the computational cost for global SA based on DGSM indices and it provides valuable information on the sensitivity of the optimal performance with respect to modeling uncertainties. This information could be used in further design steps to refine the discipline models with higher fidelity tools with respect to the most influential uncertainties on the launch vehicle performances. In the following, an application of AAO-PS and of sensitivity analysis is carried out on a Two-Stage-To-Orbit design problem to illustrate the application of the proposed methodology on a representative test case.

5. Two-stage-to-orbit test case

A case study consisting of a Two-Stage-To-Orbit (TSTO) vehicle is proposed in this section. The launch vehicle is composed of two LOx/RP-1 (Liquid Oxygen/Rocket Propellant - 1) stages and aims at delivering an 11 tons payload into a circular 400 km height orbit. The global objective to consider is the minimization of the Gross Lift-Off Weight (GLOW) of the vehicle. The first stage of the launch vehicle is composed of 9 engines. The radius at perigee of the elliptical transfer orbit for the payload injection is constrained to be above 145 km.

5.1. Definition of the disciplines and design process

From an MDO perspective, the design process is composed of the propulsion, mass/sizing, aerodynamics and trajectory disciplines. The different disciplines are described in the following. The modeling level is representative of early design phase studies of launch vehicles and allows repeated evaluations of the disciplinary models from MDO and UQ perspectives.

5.1.1. Propulsion

The propulsion discipline is based on the open-source software Chemical Equilibrium with Applications (CEA) [45] and is useful to compute the specific impulse. CEA has been developed from the 1950s at the NASA Glenn research center and allows the calculation of thermodynamic and transport properties for different mixtures of reactants. In this work, the oxidizer is assumed to be liquid oxygen (LOx) and the fuel is kerosene (RP-1). The same models are used for the first and second stages. The module is based on a set of design variables $\mathbf{z_p}$, consisting of the pressure at the combustion chamber (P_c), the pressure at the nozzle exit (P_e), the mixture ratio (O/F) and the thrust at vacuum (T_{vac}) for the first and second stages. To avoid flow separation in the first stage nozzle the value of P_{e_1} is lower bounded to 0.4 times the atmospheric pressure at sea level (Summerfield criterion [46]). Thermo-chemical equilibrium is considered in the combustion chamber and up to the throat, whereas the flow is assumed frozen in the nozzle (that is the composition does not change in the nozzle). The propulsion discipline allows the computation of the isentropic coefficient and gas molecular mass at the throat and of the combustion chamber temperature as a function of P_c and O/F. From these quantities, the specific impulse of the engines (Isp) is calculated using classical rocket propulsion equations [47]. The evaluations of CEA in the propulsion

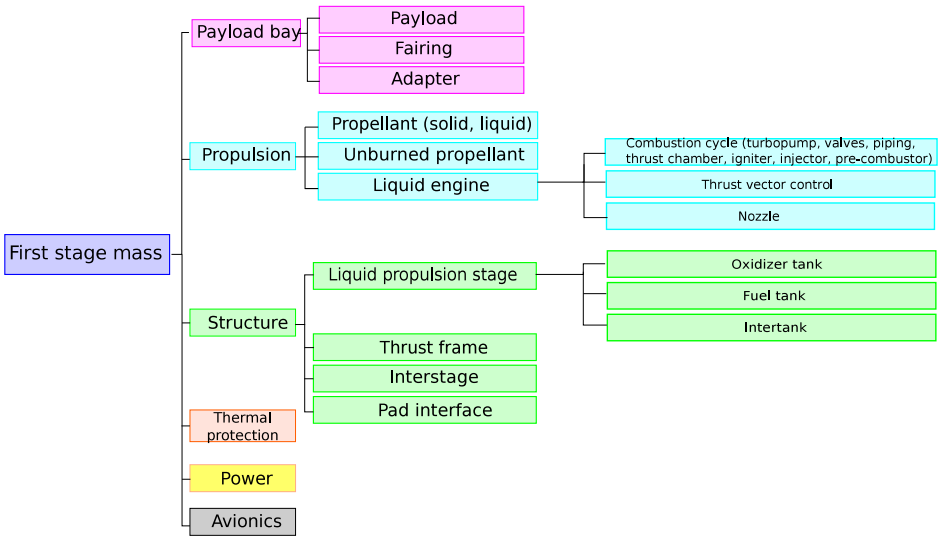

Fig. 10. Mass model derived from Castellini [48].

module are replaced by a surrogate model using a bivariate spline on a given design experiment. This approach gives access to the partial derivatives required for the optimization process. The level of accuracy of the surrogate over the entire design space allows to replace the exact model (relative error lower than 0.2% on the specific impulse between the exact model and the surrogate model).

5.1.2. Mass and sizing

The main purpose of the mass/sizing discipline is to compute the dry mass of the first and second stages. It uses the models described in Castellini [48] for the first stage and a regression model for the second stage. This discipline requires the design parameters $\mathbf{z_m}$ containing the mass of propellants of the first and second stages and the diameter of the vehicle. The considered engines correspond to gas generators. The two stages and fairing are considered to have the same diameter. The models for this discipline require as input the thrust at vacuum, which is a design variable shared among all the disciplines and the mixture ratio that is shared with the propulsion discipline. It also requires the feedback couplings with the trajectory discipline in order to design the structures according to the maximum dynamic pressure and the maximum axial load factor.

In the proposed approach, the mass/sizing discipline input coupling variables are provided by the system level optimizer along with the design variables. Additional equality constraints are added in order to ensure that at the convergence of the MDO problem, the input couplings match the output couplings given by the trajectory. The mass models for the first stage consider a cryo-storable propulsion type with RP-1 as fuel and liquid oxygen as oxidizer. The thrust frame and structures are assumed to be built in aluminum. The tanks are disposed in an "intertank" configuration. The thrust vector control is assumed to be hydraulic.

The structural mass of the first stage is modeled as a function of the mass of propellants, the mixture ratio, the stage diameter, the thrust at vacuum of the stage, the number of engines, the maximum dynamic pressure and the maximum axial load factor. The mass of the different modules (tanks, thrust frame, thrust vector control, avionics, *etc.*) are estimated using Weight Estimation Relationships (WERs) from Castellini [48]. The structural mass of the second stage relies also on WERs depending on the mass of propellants (see Fig. 10).

5.1.3. Aerodynamics

The aerodynamics model used in the design process is based on MISSILE datcom [49]. MISSILE datcom implements a large collection of analytical and semi-empirical methods encompassing a wide range of launcher configurations, geometries and flight conditions, and allowing fast estimation of launch vehicle aerodynamics coefficients. It is an adapted aerodynamics model for early design phase studies. It provides the profiles of drag and lift coefficient as a function of the angle of attack and the Mach number, and the geometry of the vehicle. These profiles are then used in the trajectory discipline to compute the drag and the lift as functions of the dynamic pressure. To do so, these profiles are interpolated using piece-wise cubic Hermite polynomial interpolation [50] in order to provide derivatives that will be used in the pseudo-spectral method for trajectory optimization.

5.1.4. Trajectory

The trajectory is modeled using Gauss–Lobatto pseudo-spectral technique using DYMOS [39], as described in Section 2.2.2. The flight is assumed to happen in the equatorial plane and is modeled in 2D polar coordinates. The jettisoning of the first stage and payload fairing for the TSTO vehicle are considered and constrained according to threshold values of dynamic pressure and heat flux. The injection into circular orbit of the payload is done using an Hohmann transfer ascent. During the trajectory, the aerodynamic loads, the drag and the lift are computed as a function of velocity and altitude, based on U.S. Standard Atmosphere models [51].

The considered equations of motion are:

$$f_{\text{ode}}: \begin{cases} \dot{r} &= v\sin(\phi) \\ \dot{\lambda} &= \frac{v\cos(\phi)}{r} \\ \dot{v} &= \frac{-D+T\cos(\theta-\phi)}{m} + \left(-g+\omega^2 r\right)\sin(\phi) \\ \dot{\phi} &= \frac{L}{mv} + \frac{T\sin(\theta-\phi)}{mv} + \frac{(\omega^2 r-g)\cos(\phi)}{v} + 2\omega + \frac{v\cos(\phi)}{r} \\ \dot{m} &= -q \end{cases} \tag{24}$$

with ω the Earth's angular velocity, λ the longitude, r the position vector from Earth's center to a fixed point in the launcher (*e.g.*, the center of gravity), θ the pitch angle, ϕ the flight path angle, α the angle of attack, m the mass of the launcher at any given time, q the mass flow rate, g the acceleration of gravity, D the drag force, L the lift force, T the thrust force and v the velocity. The trajectory is divided into four phases: lift-off, pitch-over maneuver, gravity turn and bi-linear tangent (see Fig. 11). For each part of the trajectory, specific control variables have to be defined. After the lift-off and a vertical flight (controlled by the duration of the phase $\Delta_{t_{lift-off}}$), a linear pitch-over maneuver is carried out (controlled by 3 parameters: the duration of the phase $\Delta_{t_{lpo}}$, the pitch angle target $w_{l_{po}}$, the parameter of the exponential

Table 1
Design variables for propulsion, sizing and aerodynamics.

Stage	Disciplines	Variables	Notations	Bounds	Units
1	Propulsion	Chamber Pressure	Pc_1	$[8\times10^6, 10^7]$	Pa
		Nozzle Exit Pressure	Pe_1	$[3\times10^4, 2\times10^5]$	Pa
		Oxidizer to fuel ratio	OF_1	$[2, 3]$	–
		Thrust in vacuum	T_{vac_1}	$[5\times10^6, 9\times10^6]$	N
	Sizing	Mass of propellant	Mp_1	$[200, 250]$	tons
	Aerodynamics	Stage diameter	D	$[3, 4]$	m
2	Propulsion	Chamber Pressure	Pc_2	$[8\times10^6, 10^7]$	Pa
		Nozzle Exit Pressure	Pe_2	$[10^3, 10^4]$	Pa
		Oxidizer to fuel ratio	OF_2	$[2, 3]$	–
		Thrust in vacuum	T_{vac_2}	$[8\times10^5, 10^6]$	N
	Sizing	Mass of propellant	Mp_2	$[60, 80]$	tons

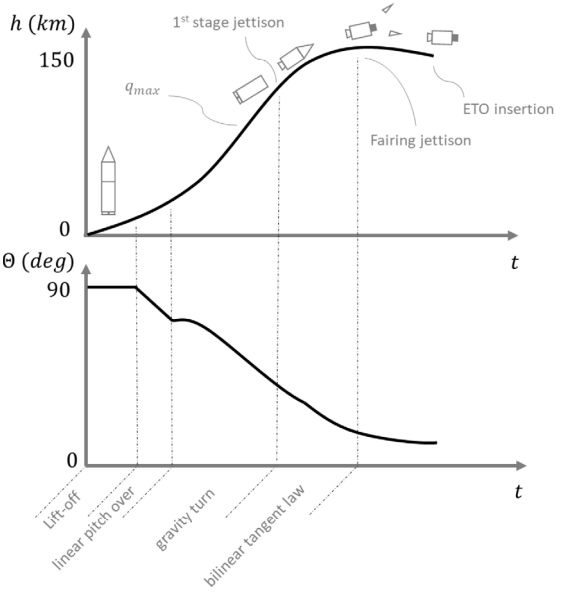

Fig. 11. Trajectory phases.

decay w_{edp}). This maneuver is composed of a linear pitch over phase Eq. (25a) and an exponential decay of the pitch angle Eq. (25b) [48]. Then, a gravity turn phase (no parameter) is involved to minimize the aerodynamics loads Eq. (25c). Once a lower threshold on the dynamic pressure is reached, this phase is followed by an exo-atmospheric phase Eq. (25d) that is parameterized by a bi-linear tangent law (3 variables $w_{blt_i}, i = 1, \ldots, 3$). For further details on the guidance for launch vehicle in MDO context, one can consult [48].

$$\theta_{lpo} = \phi + \frac{w_{lpo}}{\Delta t_{lpo}}(t_{lpo} - t_{lpo_0}) \tag{25a}$$

$$\theta_{edp} = \phi - w_{lpo} \cdot \exp\left(\frac{-3 \cdot (t_{edp} - t_{edp_0})}{w_{edp}}\right) \tag{25b}$$

$$\theta_{gt} = \phi \tag{25c}$$

$$\theta_{blt} = \arctan\left(\frac{w_{blt_1}^{w_{blt_2}} \tan\theta_{btl_0} + \left(\tan w_{blt_3} - w_{blt_1}^{w_{blt_2}} \tan\theta_{btl_0}\right)\frac{t_{btl} - t_{btl_0}}{\Delta t_{btl}}}{w_{blt_1}^{w_{blt_2}} + \left(1 - w_{blt_1}^{w_{blt_2}}\right)\frac{t_{btl} - t_{btl_0}}{\Delta t_{btl}}}\right) \tag{25d}$$

t_{x_0} is the initial time of the phase x, Δt_x the duration of the phase, t_x the current time of the phase, and θ_{x_0} the value of the pitch angle at the beginning of the phase.

5.1.5. Interdisciplinary couplings

The disciplines that have been presented in the previous section share interdisciplinary couplings. Feedforward couplings include the specific impulse (Isp) and mass flow rate thrust (q) of the stage (from propulsion to structure), length (L) and diameter (D) of the stages (from structure to aerodynamics), drag (Cx) and lift (Cz) coefficients (from aerodynamics to trajectory). Feedback couplings are composed of the maximal axial load factor (nx_{max}) and maximal dynamic pressure ($Pdyn_{max}$). These two coupling variables come from the trajectory to the structure disciplines. All the interdisciplinary couplings are summarized in Fig. 4.

5.2. Application of multidisciplinary design optimization with pseudo-spectral methods

5.2.1. Definition of the original optimization problem

The design variables that compose the design problem for Propulsion, Sizing and Aerodynamics disciplines are summarized in Table 1. The total number of design variables is 11 (6 for the first stage: diameter of the stage, chamber pressure, nozzle exit pressure, oxidizer to fuel ratio, thrust in vacuum and propellant mass, and 5 for the second stage: combustion chamber pressure, nozzle exit pressure, oxidizer to fuel ratio, thrust in vacuum, and propellant mass). The two stages share the same diameter. As described in the previous section, the launch vehicle flight is divided into four phases (see Fig. 11): vertical lift-off, the pitch-over maneuver, the gravity turn, and finally the exo-atmospheric phase with a bi-linear tangent. Four constraints are present in the optimization problem: the altitude of the apogee of the transfer orbit has to be equal to 400 km: the perigee of the transfer orbit has to be greater than 145 km; the surfaces of the first and second stages nozzle exit have to be less than a given threshold (for interstage and launch pad compatibility reasons). The objective function is the minimization of the Gross-Lift-Off-Weight (GLOW).

5.2.2. Problem formulation using MDF with direct single shooting method

The reference approach to compare the results is the MDF method using single shooting method, as it is one of the most used methods in the literature [6]. The transcription of the original problem using MDF is the following:

$$\min \; GLOW(\mathbf{z}, \mathbf{y}(\mathbf{z}, \mathbf{w})) \tag{26a}$$

$$\text{w.r.t } \mathbf{z} = \{Pc_1, Pe_1, OF_1, T_{vac_1}, Mp_1, D, Pc_2, Pe_2, OF_2, T_{vac_2}, Mp_2\}$$

$$\mathbf{w} = \{w_{lpo}, \Delta t_{lpo}, w_{edp}, w_{blt_1}, w_{blt_2}, w_{blt_3}\}$$

$$\text{s.t. } \mathbf{g}(\mathbf{z}, \mathbf{y}(\mathbf{z}, \mathbf{w})) \leq 0 \tag{26b}$$

$$\mathbf{h}(\mathbf{z}, \mathbf{y}(\mathbf{z}, \mathbf{w})) = 0 \tag{26c}$$

$$\mathbf{g}_{\text{path}}(\mathbf{z}, \mathbf{y}(\mathbf{z}, \mathbf{w}), \mathbf{x}(t), \mathbf{w}) \leq 0 \tag{26d}$$

$$\mathbf{w_{min}} \leq \mathbf{w} \leq \mathbf{w_{max}} \tag{26e}$$

with nx_{max} and $Pdyn_{max}$ the feedback coupling variables between the trajectory and the structure. These variables are handled by the MDA (Fig. 3) and consequently are functions of the optimization variables $(\mathbf{z}, \mathbf{w})$. In the implementation, the MDA involves a Gauss–Seidel algorithm [10]. $\mathbf{g}$ represents the nozzle exit area constraints, $\mathbf{g}_{\text{path}}$ is the inequality constraint about the altitude of the transfer orbit perigee, $\mathbf{h}$

Table 2
Optimal design variables for AAO and MDF.

Stages	Disciplines	Variables	Notations	MDF	AAO	Relative difference
1	Propulsion	Chamber Pressure	Pc_1	10^7	10^7	0%
		Nozzle Exit Pressure	Pe_1	5.55×10^4	5.51×10^4	0.67%
		Oxidizer to fuel ratio	OF_1	2.30	2.30	0.14%
		Thrust in vacuum	T_{vac_1}	7.10×10^6	7.12×10^6	0.24%
	Sizing	Mass of propellant	Mp_1	2.41×10^2	2.36×10^2	1.78%
	Aerodynamics	Diameter	D	3.78	3.80	0.44%
2	Propulsion	Chamber Pressure	Pc_2	10^7	10^7	0%
		Nozzle Exit Pressure	Pe_2	3.48×10^3	3.61×10^3	3.76%
		Oxidizer to fuel ratio	OF_2	2.36	2.34	0.46%
		Thrust in vacuum	T_{vac_2}	8.85×10^5	9.19×10^5	3.89%
	Sizing	Mass of propellant	Mp_2	7.18×10^4	7.53×10^4	4.93%

Table 3
Optimal coupling variables for AAO (optimization variables) and MDF (handled by the MDA).

Stages	Disciplines	Variables	Notations	MDF	AAO	Relative difference
1	Propulsion	Nozzle Exit Area	Ae_1	7.99×10^{-1}	8.04×10^{-1}	0.62%
		Mass flow rate	q_1	2.32×10^3	2.32×10^3	0.11%
		Specific impulse	Isp_1	3.12×10^2	3.12×10^2	0.01%
	Trajectory	Maximal axial load factor	nx_{max}	6.01	5.95	1.0%
		Maximal dynamic pressure	$Pdyn_{max}$	7.0×10^4	6.97×10^4	0.45%
2	Propulsion	Nozzle Exit Area	Ae_2	7.19	7.24	0.62%
		Mass flow rate	q_2	2.66×10^2	2.76×10^2	3.88%
		Specific impulse	Isp_2	3.40×10^2	3.40×10^2	0.01%

stands for the equality constraint on the transfer orbit apogee altitude. Consequently, the optimization problem to solve is composed of 16 optimization variables, three inequality constraints and one equality constraint. To perform the optimization, the system-level optimizer is based on the Covariance Matrix Adaptation – Evolution Strategy [52], that proved to be efficient to solve such a problem [53,54]. In MDF with direct single shooting method, an evolutionary algorithm is used instead of a gradient-based optimizer as the propagation of gradient through the trajectory integration (*e.g.*, using Runge–Kutta integrator in direct single shooting method) is challenging as a small modification of control law parameters may lead to a large modification of the launch vehicle states at the end of the trajectory.

5.2.3. Problem formulation using AAO with pseudo-spectral method

The transcription of the original MDO problem into an AAO formulation with pseudo-spectral method is as follows:

$$\min \; GLOW(\mathbf{z}, \mathbf{y}, \tilde{\mathbf{x}}, \tilde{\mathbf{w}}) \tag{27a}$$

$$\text{w.r.t. } \mathbf{z} = \{Pc_1, Pe_1, OF_1, T_{vac_1}, Mp_1, D, Pc_2, Pe_2, OF_2, T_{vac_2}, Mp_2\}$$

$$\mathbf{y} = \{Ae_1, Ae_2, q_1, q_2, Isp_2, nx_{max}, Pdyn_{max}\}$$

$$\tilde{\mathbf{x}} = \{\tilde{r}_k, \tilde{v}_k, \tilde{\gamma}_k, \tilde{\phi}_k, \tilde{m}_k\}$$

$$\tilde{\mathbf{w}} = \{\tilde{w}_k\}, k = 1, \ldots, M$$

$$\text{s.t. } \mathbf{g}(\mathbf{z}, \mathbf{y}, \tilde{\mathbf{x}}, \tilde{\mathbf{w}}) \leq 0 \tag{27b}$$

$$\mathbf{h}(\mathbf{z}, \mathbf{y}, \tilde{\mathbf{x}}, \tilde{\mathbf{w}}) = 0 \tag{27c}$$

$$\mathbf{y}_{ij} = \mathbf{c}_{ij}(\mathbf{z}, \mathbf{y}_{.i}, \tilde{\mathbf{x}}, \tilde{\mathbf{w}}), \forall (i,j) \in \{1, \ldots, N\}^2, i \neq j \tag{27d}$$

$$\dot{\mathcal{X}}_k(t_k, \tilde{\mathbf{x}}_k) = f_{\text{ode}}\left(\mathbf{z}, \mathbf{y}, \mathcal{X}_k(t_k, \tilde{\mathbf{x}}_k), \mathcal{W}_k(t_k, \tilde{\mathbf{w}}_k)\right) \; k = 1, \ldots, M-1 \tag{27e}$$

$$\mathbf{g}_{\text{path}}(\mathbf{z}, \mathbf{y}(\mathbf{z}), \mathcal{X}(t, \tilde{\mathbf{x}}), \mathcal{W}(t, \tilde{\mathbf{w}})) \leq 0 \tag{27f}$$

$$\mathcal{X}_{k+1}(t_k, \tilde{\mathbf{x}}_{k+1}) - \mathcal{X}_k(t_k, \tilde{\mathbf{x}}_k) = 0, \; k = 1, \ldots, M-1 \tag{27g}$$

$$\mathbf{x_{min}} \leq \mathcal{X}(t, \tilde{\mathbf{x}}) \leq \mathbf{x_{max}} \quad \forall t \in \mathcal{T} \tag{27h}$$

$$\mathbf{w_{min}} \leq \mathcal{W}(t, \tilde{\mathbf{w}}) \leq \mathbf{w_{max}} \quad \forall t \in \mathcal{T} \tag{27i}$$

$$\mathbf{x}(t_0) = \mathbf{x}_0 \tag{27j}$$

$$\mathbf{x}(t_f) = \mathbf{x}_f \tag{27k}$$

$$\mathbf{z}_{\min} \leq \mathbf{z} \leq \mathbf{z}_{\max} \tag{27l}$$

In order to decouple the different disciplines, additional coupling variables (nozzle exit area Ae, mass flow rate of the engine q, specific impulse Isp, maximal dynamic pressure $Pdyn_{max}$, maximal axial load factor nx_{max}), and corresponding coupling constraints are added. Moreover, the state and control collocation variables $\tilde{x}$ and $\tilde{w}$ are included in the optimization problem. In the same way, additional constraints related to the consistency of the trajectory are added to the original problem. Comparatively with the direct shooting MDF formulation, the number of design variables and constraints are increased. To summarize, the optimization problem to solve is of dimension 597, the number of equality constraints is 567 and the number of inequality constraints is 13. To solve this large optimization problem, a Sequential-Quadratic-Programming algorithm is used. The computation of the total derivatives of the objective and constraint functions necessary for the optimization problem solving are computed analytically based on the combination of the provided partial derivatives of the disciplinary models and the chain rule using DYMOS [39].

5.2.4. Comparative analysis

In this section, the results of the optimizations performed using the two MDO formulations (MDF and AAO) are described. The initialization point for both formulations (initial point for AAO and centroid of the CMA-ES search for MDF) is the same and is at the center of the design search domain. The optimal GLOW found by AAO is 357.9t and the optimum found by MDF is 358.3t, that represents a difference of 0.1%. Table 2 summarizes the optimal values of the design variables obtained at the convergence of the two optimization processes. The optimal configurations found by AAO and MDF are very close. The same observation can be made regarding the coupling variables as summarized in Table 3. Even if the optimal control variables present slight differences (Table 4), especially for the pitch over maneuver, the two ascent trajectories are very close, as it can be analyzed on Fig. 12 that represents the evolution of the main state variables (altitude, relative velocity, flight path and pitch angles, mass, dynamic pressure, thrust and loads) as functions of time. The differences in terms of variable values at the convergence can be explained by the fact that an evolutionary algorithm is used in MDF, and convergence of such algorithms is not defined through the satisfaction optimality conditions (Karush–Kuhn–Tucker) at the difference of the gradient-based algorithm that is used in AAO.

The performance of proposed AAO approach with respect to the reference approach can be illustrated regarding the computational time

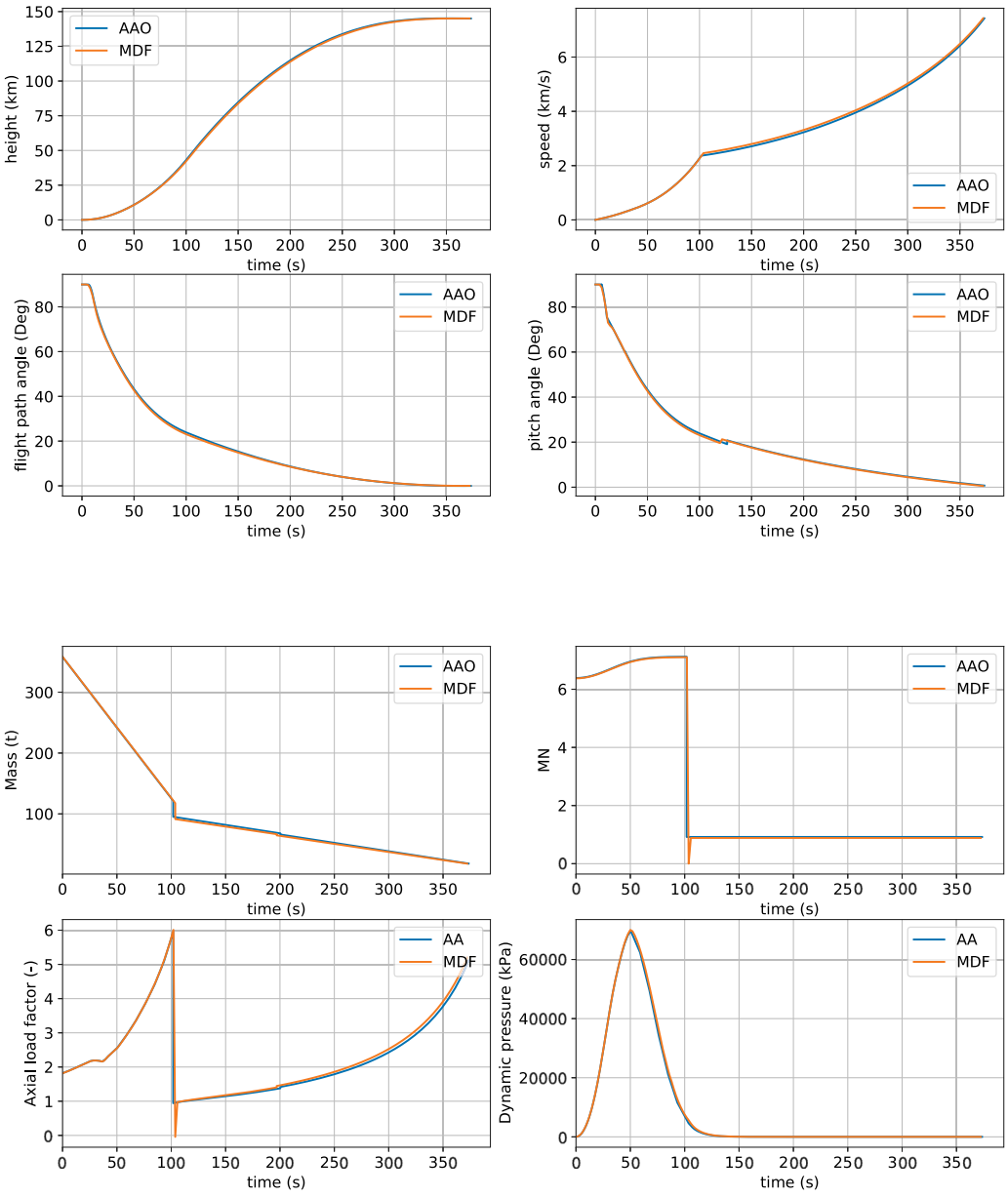

Fig. 12. Optimal trajectories (orange: MDF, blue: AAO). (For interpretation of the references to color in this figure legend, the reader is referred to the web version of this article.)

Table 4
Optimal control variables for AAO and MDF.

Stages	Variables	MDF	AAO
1	Lift-off duration (s)	5.0	6.0
	Pitch over duration (s)	7.36	5.0
	Pitch over angle (deg)	8.41	8.34
	Exponential decay duration (s)	10.0	17.0
3	Bilinear tangent initial angle (deg)	23.9	20.8
	Bilinear tangent final angle (deg)	−1.70	0.72
	Bilinear tangent form parameter (-)	−0.17	−0.13

Table 5
Computational time analysis.

	AAO	MDF
GLOW (tons)	357.9 t	358.3 t
Function evaluations	706	48000
Gradient evaluations	371	–

to obtain the optimal configuration. Indeed, the proposed method converges with 706 evaluations of the objective and constraint functions, and 371 evaluations of the gradient (Table 5). The MDF method requires 48000 evaluations of the functions to converge (corresponding to 4000 iterations of a population of 12 individuals). To this aspect, even if the problem complexity of AAO is greater in terms of dimensionality and number of constraints, the proposed method achieved to converge to a slightly better optimum than the baseline approach and with a large speed-up factor (nearly 50). The large number of evaluations in case of MDF is due to the embedded MDA process (Gauss–Seidel) inside the optimization process that takes between 3 and 4 iterations to converge at each individual proposed by the CMA-ES algorithm.

As the proposed AAO is based on a gradient-based algorithm (local search algorithm), a robustness analysis to the initialization has been carried out. For that purpose, 20 runs of AAO have been performed from random initializations over the search domain defined in Table 1. On the 20 runs, 16 have converged, that represents a success rate of 80%. The dispersion of the optimal objective functions on the

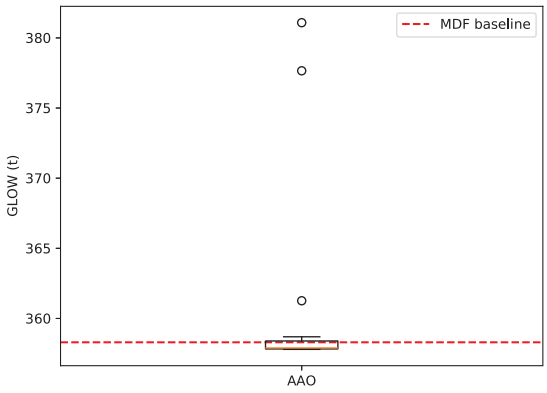

Fig. 13. Boxplot of the AAO results with 20 random initializations as an illustration of the robustness of AAO optimization with respect to the initialization (in dashed line, MDF baseline).

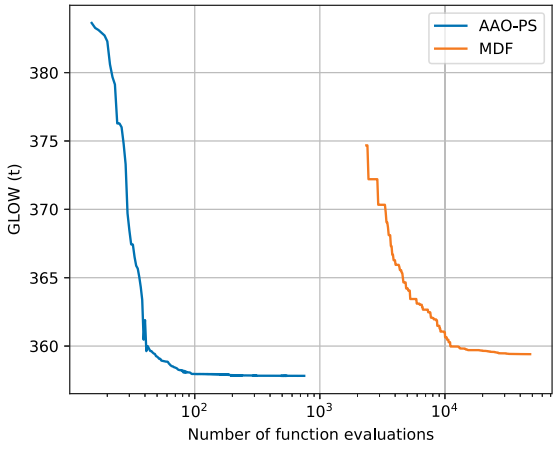

Fig. 14. Convergence curves of AAO and MDF methods (only feasible designs with respect to the constraints are depicted), for one representative AAO repetition.

converged runs is illustrated in Fig. 13, and the convergence of the methods is depicted in Fig. 14. As it can be seen, apart from 3 runs, the objective function dispersion is very small and concentrated in the region near the global optimum, illustrating the ability of AAO to find the global optimum found by using evolutionary strategy with MDF.

The trajectories obtained with AAO and MDF are depicted in Fig. 15.

5.3. Uncertainty quantification using post-optimality analysis

In this section, a sensitivity analysis is carried out to study the influence of modeling uncertainty in the early design phase on the launch vehicle optimal performances. Therefore, the proposed AAO approach is applied to uncertainty quantification analysis by calculating sensitivity analysis based on the gradient information provided by the MDO process. The efficiency of the proposed UQ analysis is linked to the efficiency of MDO solving with AAO formulation combined with post-optimal analysis and gradient-based sensitivity index estimation. First, the considered modeling uncertainties for SA are described. Then, the DGSM indices are estimated and analyzed to identify the most influential uncertain parameters on the launch vehicle performance. It allows to illustrate the ability of the proposed approach to estimate relevant sensitivity indices in a MDO context.

5.3.1. Description of uncertainties

In this section, the structure module that has been derived from Castellini [48] is assumed to present modeling uncertainties. Indeed, in the early phase design of launch vehicles, the mass balance of the

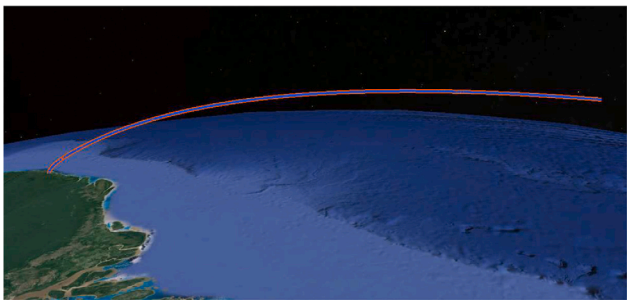

Fig. 15. Trajectories obtained with AAO (in red) and with MDF (in blue). (For interpretation of the references to color in this figure legend, the reader is referred to the web version of this article.)

launch vehicle often suffers from modeling uncertainties of the different structures of the launch vehicle. In this paper, 12 uncertain variables are considered. For the first stage, the considered uncertainties are: the oxidizer tank pressure, the fuel tank pressure, the thrust vector control system mass, the engine mass, the avionic system mass, the thrust frame mass, the thermal protection system mass, the intertank mass, the electrical and power system mass and the unburnt propellant at the end of the launch vehicle flight. For the second stage, two uncertain parameters are considered: the unburnt propellant and the stage dry mass estimation. Table 6 summarizes the uncertain variables and the associated distribution laws given by expert knowledge.

5.3.2. Results synthesis

As it is mentioned in the previous section, to perform sensitivity analysis on the optimal objective function considering the uncertain variables, it is required to compute the gradient of the objective function with respect to the uncertain variables. Unfortunately, as these variables are not optimization variables, direct calculation is not possible and in the proposed approach a Post-Optimality Analysis (POA) is carried out. To validate the results provided by POA, a comparison has been performed with respect to finite difference calculations. The results of this comparative analysis are summarized in Fig. 16. The derivative estimations provided by POA are very accurate (the largest relative difference is 0.014% on the avionics mass uncertainty, see Table 7). It is interesting to note that the POA only requires one solving of the MDO problem with AAO formulation to estimate all the derivatives whereas the finite difference scheme requires 13 MDO problem solvings. This speed-up factor is directly proportional to the number of considered uncertainties.

The first order and second order DGSM indices are depicted in Fig. 16. For the calculation of the sensitivity indices, a Monte Carlo analysis is carried out with 5000 realizations of uncertainties to compute the integrals involved in the DGSM. The ranking obtained by taking into account either the first or the second order DGSM is the same. The higher indices are obtained for the uncertainties considering the unburnt propellant of stages 1 and 2. The sensitivity associated to the second stage unburnt propellant is the most influential due to the fact that this unburnt propellant is analog to an additional payload mass that has to be injected into orbit whereas the unburnt propellant of the first stage is jettisoned during the flight. Then, the uncertainties about the TVC mass, the engine mass, the avionics mass, the thrust frame mass, the thermal protection mass, the electric power system mass and the intertank mass seem to have a quite equivalent impact on the output using DGSM. Finally, the uncertainties associated to the tank masses (stage 1 and 2) are the less sensitive ones. This sensitivity analysis is useful to detect which sub-model about the mass balance is the most influential with respect to the performance of the designed architecture. This allows to identify the effort to put on the refinement of the mass sub-model in order to increase the robustness of the optimal

Table 6
Signification of uncertainties and probabilistic modeling.

	Signification	*Name*	*Probability law*
Stage 1	Oxidizer tank pressure	$u_{P_{ox}}$	$\mathcal{N}(3, 0.05)$
	Fuel tank pressure	u_{P_f}	$\mathcal{N}(3, 0.05)$
	Thrust vector control system mass	u_{TVC}	$\mathcal{N}(0, 10)$
	Engine mass	u_{eng}	$\mathcal{N}(0, 20)$
	Avionics system mass	u_{avio}	$\mathcal{N}(0, 10)$
	Thrust frame mass	u_{TF}	$\mathcal{N}(0, 50)$
	Thermal protection system mass	u_{TPS}	$\mathcal{N}(0, 20)$
	Intertank mass	u_{int}	$\mathcal{N}(0, 15)$
	Electrical and power system mass	u_{EPS}	$\mathcal{N}(0, 10)$
	Unburnt propellant amount	u_{unb_1}	$\mathcal{N}(1, 0.001)$
Stage 2	Unburnt propellant amount	u_{unb_2}	$\mathcal{N}(1, 0.001)$
	Global dry mass uncertainty	u_{dm_2}	$\mathcal{N}(1, 50)$

Table 7
Validation of Post optimality analysis : Comparison of finite difference scheme (requiring 13 optimizations) and post optimality analysis (requiring 1 optimization).

Type of uncertainty	*Finite differences*	*Post Optimality Analysis*	*Relative difference (in %)*
Oxydizer tank pressure	3.7137×10^{-3}	3.7134×10^{-3}	7.30×10^{-3}
Fuel tank pressure	2.7280×10^{-3}	2.7273×10^{-3}	2.31×10^{-3}
TVC mass	2.9062×10^{1}	2.9063×10^{1}	-9.62×10^{-4}
Engine mass	3.1725×10^{1}	3.1725×10^{1}	-1.29×10^{-3}
Avionics system mass	4.9286×10^{0}	4.9293×10^{0}	-1.40×10^{-2}
Thrust frame mass	3.2289×10^{0}	3.2292×10^{0}	-9.19×10^{-3}
Unburnt propellant mass stage 1	1.1627×10^{4}	1.1627×10^{4}	4.37×10^{-4}
Unburnt propellant mass stage 2	7.4172×10^{4}	7.4173×10^{4}	-6.06×10^{-4}
Dry mass stage 2	2.2107×10^{1}	2.2107×10^{1}	-7.59×10^{-5}
TPS mass	3.8654×10^{0}	3.8654×10^{0}	-6.27×10^{-6}
EPS mass	1.6106×10^{0}	1.6106×10^{0}	-6.32×10^{-5}
Intertank mass	1.0630×10^{0}	1.0630×10^{0}	2.89×10^{-5}

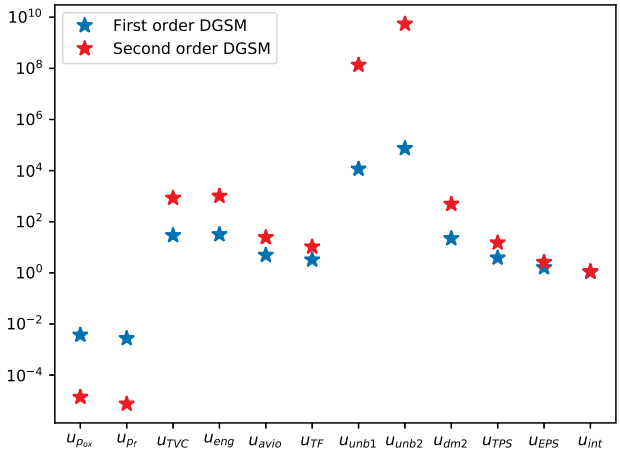

Fig. 16. First order and second order DGSM indices.

solution founds in early design phases. In that case, the corresponding model needs to be refined with respect to identification of the unburnt masses of propellant which have a predominant effect. To the contrary, the tank pressures could be fixed to their mean values as their effects are very small on the overall launch vehicle performance.

6. Conclusions

In this paper, a MDO formulation dedicated to launch vehicle design has been proposed to deal with the specificity of the optimal control problem involved in the trajectory design discipline. It combines the All-At-Once (AAO) decoupled formulation and a pseudo-spectral decomposition (with Gauss–Lobatto collocation) of the trajectory optimal control problem. Compared to traditional Multi Discipline Feasible (MDF) formulation which results in a three layers nested loop (system-level optimizer, MultiDisciplinary Analysis and trajectory optimization), the proposed approach exploits the commonalities of AAO and pseudo-spectral techniques regarding the decoupling of the optimization problem. This enables the use of gradient-based optimizers to provide efficient convergence properties. In addition, a Sensitivity Analysis technique in the context of MDO problem has been proposed by combining the AAO formulation and post-optimality Analysis to estimate derivative-based global sensitivity measures indices. This allows to analyze the influence of modeling uncertainty on the optimal launch vehicle performance in the early design phases. The proposed approach has been applied on a representative Two-Stage-To-Orbit (TSTO) design test case illustrating the efficiency of the proposed AAO formulation compared to traditional MDF. Moreover, the sensitivity analysis allows to identify the most influential modeling uncertainties of the optimal TSTO performances providing modeling refinement perspectives. In future work, the proposed approach could be applied to higher fidelity models and more complex launch vehicle design problems.

Declaration of competing interest

The authors declare that they have no known competing financial interests or personal relationships that could have appeared to influence the work reported in this paper.

Acknowledgments

The uncertainty propagation study has been performed using the OpenTURNS library [55]. The design process has been built using OpenMDAO library [40] and the trajectory transcription with pseudo-spectral technique has been done with DYMOS library [39].

References

[1] M. Balesdent, Multidisciplinary design optimization of launch vehicles (Ph.D. thesis), Ecole Centrale de Nantes, 2011.
[2] M. Cerf, Optimal injection point for launch trajectories with parametric thrust profile, Acta Astronaut. 151 (2018) 752–760.

[3] J.T. Betts, Survey of numerical methods for trajectory optimization, J. Guid. Control Dyn. 21 (2) (1998) 193–207.
[4] J.T. Betts, Practical Methods for Optimal Control and Estimation using Nonlinear Programming, SIAM, 2010.
[5] A.V. Rao, A survey of numerical methods for optimal control, Adv. Astronaut. Sci. 135 (1) (2009) 497–528.
[6] M. Balesdent, N. Bérend, P. Dépincé, A. Chriette, A survey of multidisciplinary design optimization methods in launch vehicle design, Struct. Multidiscip. Optim. 45 (5) (2012) 619–642.
[7] J.R. Martins, A.B. Lambe, Multidisciplinary design optimization: a survey of architectures, AIAA J. 51 (9) (2013) 2049–2075.
[8] R.J. Balling, J. Sobieszczanski-Sobieski, Optimization of coupled systems-a critical overview of approaches, AIAA J. 34 (1) (1996) 6–17.
[9] L. Brevault, M. Balesdent, S. Defoort, Preliminary study on launch vehicle design: Applications of multidisciplinary design optimization methodologies, Concurr. Eng. 26 (1) (2018) 93–103.
[10] L. Brevault, M. Balesdent, J. Morio, Aerospace System Analysis and Optimization in Uncertainty, Springer, 2020.
[11] R. Ghanem, D. Higdon, H. Owhadi, et al., Handbook of Uncertainty Quantification, Vol. 6, Springer, 2017.
[12] S. Da Veiga, F. Gamboa, B. Iooss, C. Prieur, Basics and Trends in Sensitivity Analysis: Theory and Practice in R, SIAM, 2021.
[13] M.D. Morris, Factorial sampling plans for preliminary computational experiments, Technometrics 33 (2) (1991) 161–174.
[14] I. Sobol', Sensitivity estimates for nonlinear mathematical models, Math. Model. Comput. Exp. 1 (4) (1993) 407–414.
[15] S. Da Veiga, Global sensitivity analysis with dependence measures, J. Stat. Comput. Simul. 85 (7) (2015) 1283–1305.
[16] B. Iooss, P. Lemaître, A review on global sensitivity analysis methods, in: Uncertainty Management in Simulation-Optimization of Complex Systems, Springer, 2015, pp. 101–122.
[17] S. Kucherenko, S. Song, Derivative-based global sensitivity measures and their link with Sobol'sensitivity indices, in: Monte Carlo and Quasi-Monte Carlo Methods, Springer, 2016, pp. 455–469.
[18] J. Sobieszczanski-Sobieski, Sensitivity analysis and multidisciplinary optimization for aircraft design-recent advances and results, J. Aircr. 27 (12) (1990)) 993–1001.
[19] L.S. Pontryagin, Mathematical Theory of Optimal Processes, CRC Press, 1987.
[20] M. Cerf, Versatile launcher preliminary design, J. Spacecr. Rockets 56 (2) (2019) 517–525.
[21] F. Bonnans, E. Casas, An extension of Pontryagin's principle for state-constrained optimal control of semilinear elliptic equations and variational inequalities, SIAM J. Control Optim. 33 (1) (1995) 274–298.
[22] R.D. Falck, J.S. Gray, Optimal control within the context of multidisciplinary design, analysis, and optimization, in: AIAA Scitech 2019 Forum, 2019, p. 0976.
[23] I.M. Ross, M. Karpenko, A review of pseudospectral optimal control: From theory to flight, Annu. Rev. Control 36 (2) (2012) 182–197.
[24] E.J. Cramer, J.E. Dennis Jr., P.D. Frank, R.M. Lewis, G.R. Shubin, Problem formulation for multidisciplinary optimization, SIAM J. Optim. 4 (4) (1994) 754–776.
[25] C. Dupont, A. Tromba, S. Missonnier, New strategy to preliminary design space launch vehicle based on a dedicated MDO platform, Acta Astronaut. 158 (2019) 103–110.
[26] M.A. Lobbia, Multidisciplinary design optimization of waverider-derived crew reentry vehicles, J. Spacecr. Rockets 54 (1) (2017) 233–245.
[27] D. Zhang, Y. Zhang, Multidisciplinary design and optimization of an innovative nano air launch vehicle with a twin-fuselage UAV as carrier aircraft, Acta Astronaut. 170 (2020) 397–411.
[28] T. Zhang, X. Yan, W. Huang, X. Che, Z. Wang, Multidisciplinary design optimization of a wide speed range vehicle with waveride airframe and RBCC engine, Energy 235 (2021) 121386.
[29] N. Duranté, A. Dufour, V. Pain, G. Baudrillard, M. Schoenauer, Multi-disciplinary analysis and optimisation approach for the design of expendable launchers, in: 10th AIAA/ISSMO Multidisciplinary Analysis and Optimization Conference, 2004, p. 4441.
[30] S. Akhtar, H. Linshu, Simulation-based optimization strategy for liquid fueled multi-stage space launch vehicle, in: Sixth International Conference on Parallel and Distributed Computing Applications and Technologies (PDCAT'05), IEEE, 2005, pp. 359–365.
[31] M. Ebrahimi, M.R. Farmani, J. Roshanian, Multidisciplinary design of a small satellite launch vehicle using particle swarm optimization, Struct. Multidiscip. Optim. 44 (6) (2011) 773–784.
[32] T. Fujikawa, T. Tsuchiya, S. Tomioka, Multidisciplinary design optimization of a two-stage-to-orbit reusable launch vehicle with ethanol-fueled rocket-based combined cycle engines, Trans. Japan Soc. Aeronaut. Space Sci. 60 (5) (2017) 265–275.
[33] R. Balling, C. Wilkinson, Execution of multidisciplinary design optimization approaches on common test problems, AIAA J. 35 (1) (1997) 178–186.
[34] R. Braun, R. Powell, R. Lepsch, D. Stanley, I. Kroo, Comparison of two multidisciplinary optimization strategies for launch-vehicle design, J. Spacecr. Rockets 32 (3) (1995) 404–410.
[35] M. Tava, Integrated multidisciplinary and multicriteria optimization of a space transportation system and its trajectory, in: 54th International Astronautical Congress of the International Astronautical Federation, 2003, U–3.
[36] N.F. Brown, J.R. Olds, Evaluation of multidisciplinary optimization techniques applied to a reusable launch vehicle, J. Spacecr. Rockets 43 (6) (2006) 1289–1300.
[37] A. Adami, M. Mortazavi, M. Nosratollahi, A new approach in multidisciplinary design optimization of upper-stages using combined framework, Acta Astronaut. 114 (2015) 174–183.
[38] T. Fujikawa, T. Tsuchiya, S. Tomioka, Multi-objective, multidisciplinary design optimization of TSTO space planes with RBCC engines, in: 56th AIAA/ASCE/AHS/ASC Structures, Structural Dynamics, and Materials Conference, 2015, p. 0650.
[39] R. Falck, J.S. Gray, K. Ponnapalli, T. Wright, Dymos: A Python package for optimal control of multidisciplinary systems, J. Open Source Softw. 6 (59) (2021) 2809, http://dx.doi.org/10.21105/joss.02809.
[40] J.S. Gray, J.T. Hwang, J.R.R.A. Martins, K.T. Moore, B.A. Naylor, OpenMDAO: An open-source framework for multidisciplinary design, analysis, and optimization, Struct. Multidiscip. Optim. 59 (4) (2019) 1075–1104, http://dx.doi.org/10.1007/s00158-019-02211-z.
[41] A. Kiparissides, S. Kucherenko, A. Mantalaris, E. Pistikopoulos, Global sensitivity analysis challenges in biological systems modeling, Ind. Eng. Chem. Res. 48 (15) (2009) 7168–7180.
[42] W. Karush, Minima of functions of several variables with inequalities as side constraints, (M. Sc. Dissertation), Dept. of Mathematics, Univ. of Chicago, 1939.
[43] R. Braun, I. Kroo, P. Gage, Post-optimality analysis in aerospace vehicle design, in: Aircraft Design, Systems, and Operations Meeting, 1993, p. 3932.
[44] I.R. Chittick, J.R. Martins, Aero-structural optimization using adjoint coupled post-optimality sensitivities, Struct. Multidiscip. Optim. 36 (1) (2008) 59–70.
[45] S. Gordon, B. McBride, NASA computer program chemical equilibrium with applications (CEA), NASA RP-1311 Part 1 (1994).
[46] M. Summerfield, A theory of unstable combustion in liquid propellant rocket systems, J. Am. Rocket Soc. 21 (5) (1951) 108–114.
[47] W.J. Larson, G.N. Henry, R.W. Humble, Space Propulsion Analysis and Design, McGraw-Hill, 1995.
[48] F. Castellini, Multidisciplinary design optimization for expendable launch vehicles, 2012.
[49] W.B. Blake, Missile datcom: User's manual-1997 FORTRAN 90 revision, Technical report, Air Force Research Lab Wright-Patterson AFB OH Air Vehicles Directorate, 1998.
[50] F.N. Fritsch, R.E. Carlson, Monotone piecewise cubic interpolation, SIAM J. Numer. Anal. 17 (2) (1980) 238–246.
[51] A.J. Krueger, R.A. Minzner, A mid-latitude ozone model for the 1976 US standard atmosphere, J. Geophys. Res. 81 (24) (1976) 4477–4481.
[52] N. Hansen, S.D. Müller, P. Koumoutsakos, Reducing the time complexity of the derandomized evolution strategy with covariance matrix adaptation (CMA-ES), Evol. Comput. 11 (1) (2003) 1–18.
[53] L. Brevault, M. Balesdent, Multidisciplinary system modeling and optimization, in: Aerospace System Analysis and Optimization in Uncertainty, Springer, 2020, pp. 3–30.
[54] L. Brevault, M. Balesdent, A. Hebbal, Expendable and reusable launch vehicle design, in: Aerospace System Analysis and Optimization in Uncertainty, Springer, 2020, pp. 421–476.
[55] M. Baudin, A. Dutfoy, B. Iooss, A.-L. Popelin, Open TURNS: An industrial software for uncertainty quantification in simulation, 2015, arXiv preprint arXiv:1501.05242.